Journal of African Earth Sciences 61 (2011) 167–232

Contents lists available at SciVerse ScienceDirect

Journal of African Earth Sciences

journal homepage: www.elsevier.com/locate/jafrearsci

Late Cryogenian–Ediacaran history of the Arabian–Nubian Shield: A review of depositional, plutonic, structural, and tectonic events in the closing stages of the northern East African Orogen

P.R. Johnson [a,*], A. Andresen [b], A.S. Collins [c], A.R. Fowler [d], H. Fritz [e], W. Ghebreab [f], T. Kusky [g], R.J. Stern [h]

[a] 6016 SW Haines Street, Portland, OR 97219, USA
[b] Department of Geosciences, University of Oslo, P.O. Box 1047, Blindern 0316, Oslo, Norway
[c] Tectonics Resources and Exploration (TRaX), Geology and Geophysics, School of Earth and Environmental Sciences, The University of Adelaide, Adelaide, SA 5005, Australia
[d] Geology Department, Faculty of Sciences, United Arab Emirates University, P.O. Box 17551, Al-Ain, Abu Dhabi, United Arab Emirates
[e] Department of Earth Sciences, University of Graz, Heinrichstraße 26, A-8010 Graz, Austria
[f] Columbus State Community College, Department of Physical Sciences NH425, 550 East Spring Street, Columbus, OH 43215, USA
[g] State Key Laboratory of Geological Processes and Mineral Resources, Three Gorges Research Center for Geohazards, China University of Geosciences, Wuhan, China
[h] Geosciences Department, University of Texas at Dallas, Richardson, TX 75080-0688, USA

ARTICLE INFO

Article history:
Received 15 February 2011
Received in revised form 1 July 2011
Accepted 9 July 2011
Available online 23 July 2011

Keywords:
Arabian–Nubian Shield
Cryogenian
Ediacaran
Tectonics
Magmatism
Deposition

ABSTRACT

During the late Cryogenian–Ediacaran (650–542 Ma), the Arabian–Nubian Shield (ANS) underwent final assembly and accretion to the Saharan Metacraton concurrent with the assembly of eastern and western Gondwana. At the end of the Precambrian it lay at one end of the East African Orogen, with its northern margin (present coordinates) forming a low-relief stable shelf facing an open ocean; to the south the ANS transitioned into the Mozambique Belt. The geologic history of the ANS during this period provides insight into the closing developmental stages of one of the world's largest accretionary orogens. Following a 680–640 Ma orogenic event reflecting amalgamation of a core grouping of island-arc terranes (the proto-Arabian–Nubian Shield; pANS), the region underwent extensive exhumation, erosion, and subsidence. Depositional basins formed in the northern and eastern pANS, with those in the east below sea level and connected to an ocean. Periodic basin closure and formation of new basins in other parts of the ANS followed. Many basins were filled by terrestrial, molasse-type sediments interfingering with subordinate to predominant amounts of volcanic rocks. Magmatism was extensive throughout the period, initially characterized by tonalite–trondhjemite–granodiorite (TTG) and granite (monzogranite, syenogranite), but also characterized, from ~610 Ma on, by increasing amounts of alkali-feldspar granite and alkali granite. The plutons are largely undeformed, except where cut by brittle–ductile shear zones. The magma sources of the late Cryogenian–Ediacaran granitoids were dominated by juvenile crust and(or) depleted mantle and magmas mostly originated in anorogenic, post-collisional, commonly extensional, settings. They were derived by melting and fractionation of anhydrous high-grade metamorphosed lower crust, mafic- to intermediate calc-alkaline crust, and(or) subduction-modified mantle wedges associated with slab break-off or delamination.

By ~630 Ma, the region was affected by oblique (transpressional) convergence of continental blocks that formed eastern and western Gondwana—the pANS was approaching the Saharan Metacraton; north-trending shear and shortening zones developed in the southern ANS; and northwest-trending strike-slip shear zones of the Najd fault system dominated farther north. In the northwestern ANS, convergence and Najd transpression buckled the crust causing structural highs with domes of gneissic infracrust overlain by supracrust composed of ophiolitic and volcanosedimentary assemblages dating from the Tonian–middle Cryogenian period of island-arc activity. The supracrust was extensively translated to the northwest above a high-strain zone. Extension and tectonic escape augmented exhumation of the gneissic infracrust particularly between ~620–580 Ma. In the northeastern ANS, linear belts of gneiss formed from reworked older intrusive bodies or syntectonic intrusions that were emplaced along Najd faults. By ~620 Ma a marine basin on the eastern margin of the pANS (present coordinates) was beginning to close. A thick sedimentary assemblage (Abt formation) in this basin underwent metamorphism and folding, and subduction-related magmatism and volcanism farther into this basin (Al Amar arc; >690–615 Ma) was coming to an end. Amalgamation of the Abt formation, Al Amar arc, and the pANS

* Corresponding author.
E-mail address: petergeo@earthlink.net (P.R. Johnson).

1464-343X/$ - see front matter
doi:10.1016/j.jafrearsci.2011.07.003

occurred between ~620 and ~605 Ma, and terminal collision between the pANS and the Saharan Metacraton was complete by ~580 Ma. At this time, the ANS was fully assembled. Granite magmatism continued until ~565–560 Ma and orogeny ceased by ~550 Ma. During these terminal events, the region underwent strong chemical weathering and became a vast low-relief surface on which Lower Paleozoic sandstone was eventually deposited.

1. Introduction and geologic setting

This paper reviews the closing 100 million years of crustal growth in the Arabian–Nubian Shield (ANS), covering the period between 650 Ma and 542 Ma, and describes the late Cryogenian–Ediacaran depositional, structural, metamorphic, intrusive, and mineralization events involved in the final stages of the development of the northern part of the East African Orogen (EAO). The ANS is a collage of Neoproterozoic juvenile arcs, younger sedimentary and volcanic basins, voluminous granitoid intrusions, and enclaves of pre-Neoproterozoic crust that crop out in the western Arabian Plate and the northeastern African Plate (Fig. 1) at the northern end of the EAO (Stern, 1994; Kusky et al., 2003; Johnson and Woldehaimanot, 2003) (Fig. 2). Differences in the orientation of structural trends divide the shield into southern and northern parts. Prior to Red Sea-Gulf of Aden opening (beginning ~25 Ma), the Arabian and Nubian Shields were conjoined as one of the largest tracts of juvenile Neoproterozoic crust on Earth. The review period is bracketed by (1) the Tonian–middle Cryogenian development and amalgamation of island-arc terranes to form the core of what is now the ANS, and (2) the end-Precambrian conversion of the ANS into stable shield and its superimposition by a vast Lower Paleozoic siliciclastic blanket deposited above a regional unconformity developed on the newly created shield.

In a larger context, the events reviewed here are part of an orogenic cycle extending from the breakup of Rodinia (870–800 Ma) (Li et al., 2007) to the final amalgamation of Gondwana (Fig. 3) in the Cambrian (Li and Powell, 1993; Collins and Pisarevsky, 2005; Pisarevsky et al., 2008). Topics considered include: (1) the deposition of volcanosedimentary sequences in post-amalgamation basins unconformable on newly amalgamated island-arc rocks; (2) the emplacement of large volumes of granitic rock in the newly amalgamated island-arc terranes and the post-amalgamation basins; (3) the effects of transpression, transtension, uplift, and exhumation associated with orogenic collapse and tectonic escape, reflecting an interplay between compression and extension related to far-field movements of crustal blocks involved in the coalescence of Gondwana; and (4) periods of major erosion. Many of the late Cryogenian–Ediacaran events in this cycle have been individually described and interpreted in the geologic literature. Our aim in this contribution is to present an integrated geologic history, describing interrelated features during an important tectonic period in Earth history.

During the late Cryogenian and Ediacaran, the Earth was affected by major climatic changes evidenced by glaciation and isotopic excursions (Hoffman et al., 1998; Halverson et al., 2010; Fike et al., 2006; Hurtgen et al., 2006). It underwent a dramatic development of multicellular organisms augmenting a biosphere that, until the Ediacaran, was dominated by single-celled organisms best preserved as stromatolites, and it witnessed the growth of the longest-lived supercontinent of all time–Gondwana—that resulted from the assembly of crustal blocks derived from the earlier break-up of the Rodinia supercontinent and other independent continental blocks and the closure of the Mozambique and other oceans (Meert, 2002; Boger and Miller, 2004; Collins and Pisarevsky, 2005; Li et al., 2007; Meert and Lieberman, 2008; Pisarevsky et al., 2008). The ANS is a key part of this larger history having originated by subduction and island-arc development in the Mozambique Ocean, and ending as part of an orogenic belt caught up between converging Gondwanan blocks.

1.1. East African Orogen and the margins of ANS

The EAO (Stern, 1994; Kusky et al., 2003) (Fig. 2) consists of deformed and metamorphosed rocks of the ANS in the north and higher grade and more strongly deformed rocks of East Africa and Madagascar in the south. A southern continuation, through Mozambique into Antarctica, proposed by Jacobs and Thomas (2004), was challenged by Collins and Pisarevsky (2005). Here we use the original definition of the orogen and limit its southern extent to the northern Mozambique/Madagascar region where a western arm links with the Zambezi Belt (Johnson et al., 2005) and an eastern arm heads through southern India and Sri Lanka to enter East Antarctica in the region of Lutzow-Holm Bay (Collins and Pisarevsky, 2005). The geology of the East African part of the EAO is the subject of a forthcoming review by Fritz and colleagues.

The EAO is an extensive Neoproterozoic accretionary orogen and collisional zone within Gondwana (Stern, 1994; Collins and Windley, 2002; Cawood et al., 2009). Following the determination of a U–Pb age of 652 ± 10 Ma for zircons in garnet-bearing two-pyroxene granulite in Tanzania (Coolen et al., 1982), it was realized that high-grade metamorphism in East Africa was a Neoproterozoic, not an older event, despite the Mesoproterozoic to Archean protolith ages of some of the rocks caught up in the orogen (see geochronologic reviews by Möller et al. (1998), and Tenczer et al. (2006)). Greenwood et al. (1980) extended the Mozambique Belt northward into the ANS and Berhe (1990) described ANS-type ophiolite-decorated north-trending shear zones extending S into central Kenya, confirming that the Mozambique Belt and the Arabian–Nubian Shield are correlatives. Profound differences in lithology, structure, metamorphic grade, and tectonic history make detailed correlation challenging and intervening cover interrupts direct continuity. However, the link between the two regions is evidenced between southern Ethiopia and southern Kenya (Fig. 2). In southern Ethiopia, low-grade Neoproterozoic basement rocks of the Arabian–Nubian Shield structurally overly high-grade granitic migmatite of the Mozambique Belt (Yihunie and Tesfaye, 2002). Similar juxtaposition of high- and low-grade rocks is found in the Bulbul Belt, southern Ethiopia as a SE-dipping, top-to-the-SE, low-angle shear zone that developed during regional gravitational tectonic collapse (Tsige and Abdelsalam, 2005). In southern Kenya Neoproterozoic volcanic and sedimentary rocks occur between prominent ophiolite-decorated shear zones. The northwest-trending sinistral Aswa shear zone in the west contains the Seker ophiolite; the north-trending dextral Barsaloi shear zone in the center contains the Barsaloi ophiolite; and the curved, north-trending dextral Mutito shear zone in the east, contains the Moyale ophiolite.

In contrast to the ANS, the orogen in East Africa and Madagascar includes large amounts of Archean to Mesoproterozoic rocks that were reworked during Neoproterozoic metamorphism and anatexis, as well as subordinate amounts of juvenile Neoproterozoic igneous rocks. End-Precambrian extension and exhumation was intense in the S and the EAO exposures in East Africa are commonly

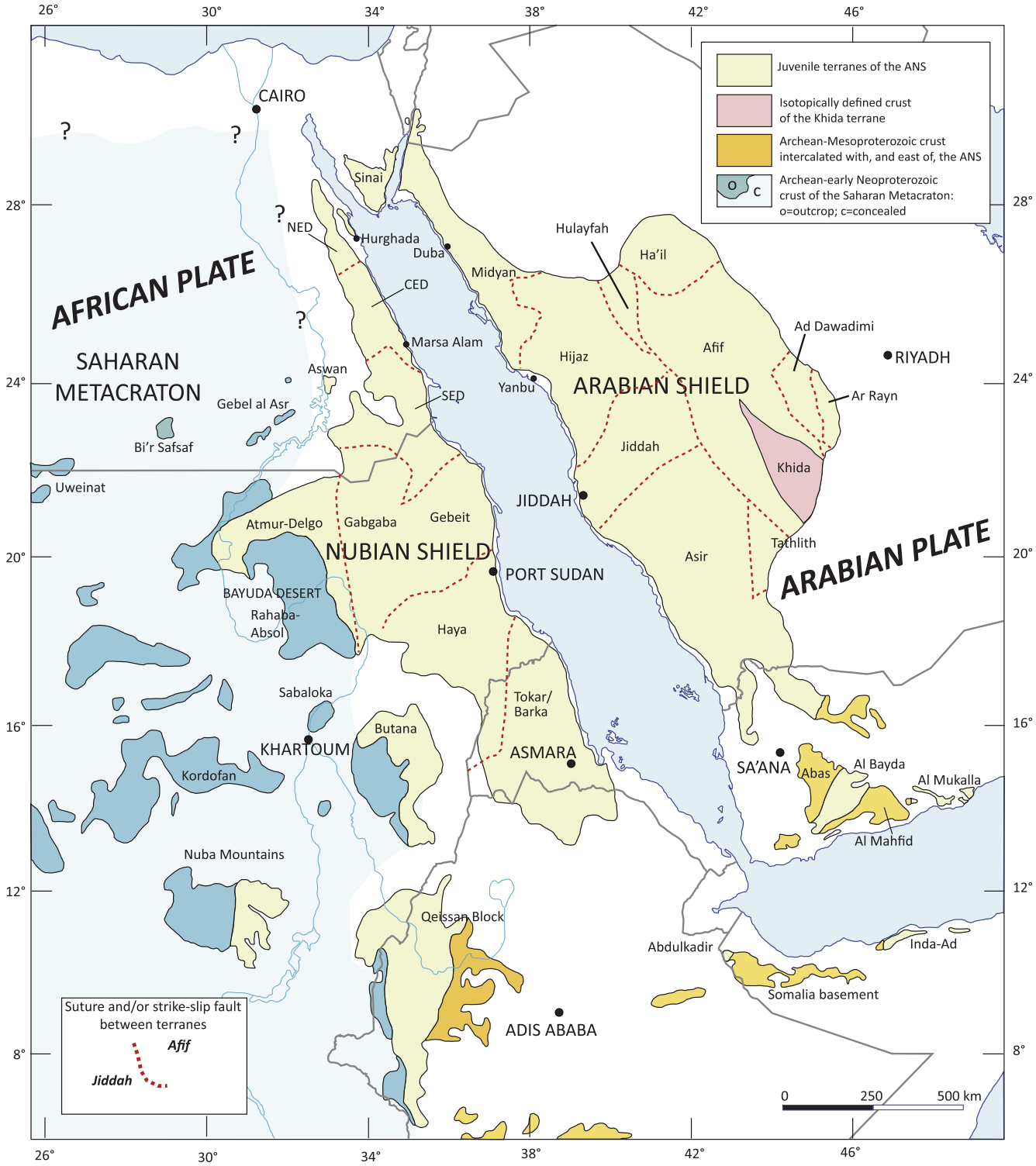

Fig. 1. The Arabian–Nubian Shield (ANS), showing its relationship to adjacent areas of older continental crust. The border with the Saharan Metacraton, on the west, is the effective contact between ANS and West Gondwana: a border, on the east, with putative East Gondwanan crust, is not certain. NED = North Eastern Desert; CED = Central Eastern Desert; SED = South Eastern Desert. In this and other figures, Tokar/Barka is a composite term for terranes in Eritrea (see Drury and de Souza Filho, 1998).

amphibolite- and granulite-facies schists and gneisses in contrast to the greenschist-facies rocks prevalent in the ANS, implying greater uplift and erosion southward. Another difference is that orogeny persisted longer in the south than in the north and continued into the early Cambrian (Bingen et al., 2009). Nonetheless, both regions are parts of a common orogenic belt affected by periods of E–W directed shortening generated by the closure of the Mozambique Ocean and the ultimate collision of Neoproterozoic India with the Congo–Tanzania–Bangweulu Block (in the south) and the Sahara Metacraton (in the north). The entire orogen remained intact until the dispersal of Gondwana in the Early to Middle Jurassic, and is now represented by fragments of Neoproterozoic–Cambrian deformed and metamorphosed rocks preserved in the Arabian, African, Madagascan, and Indian Plates.

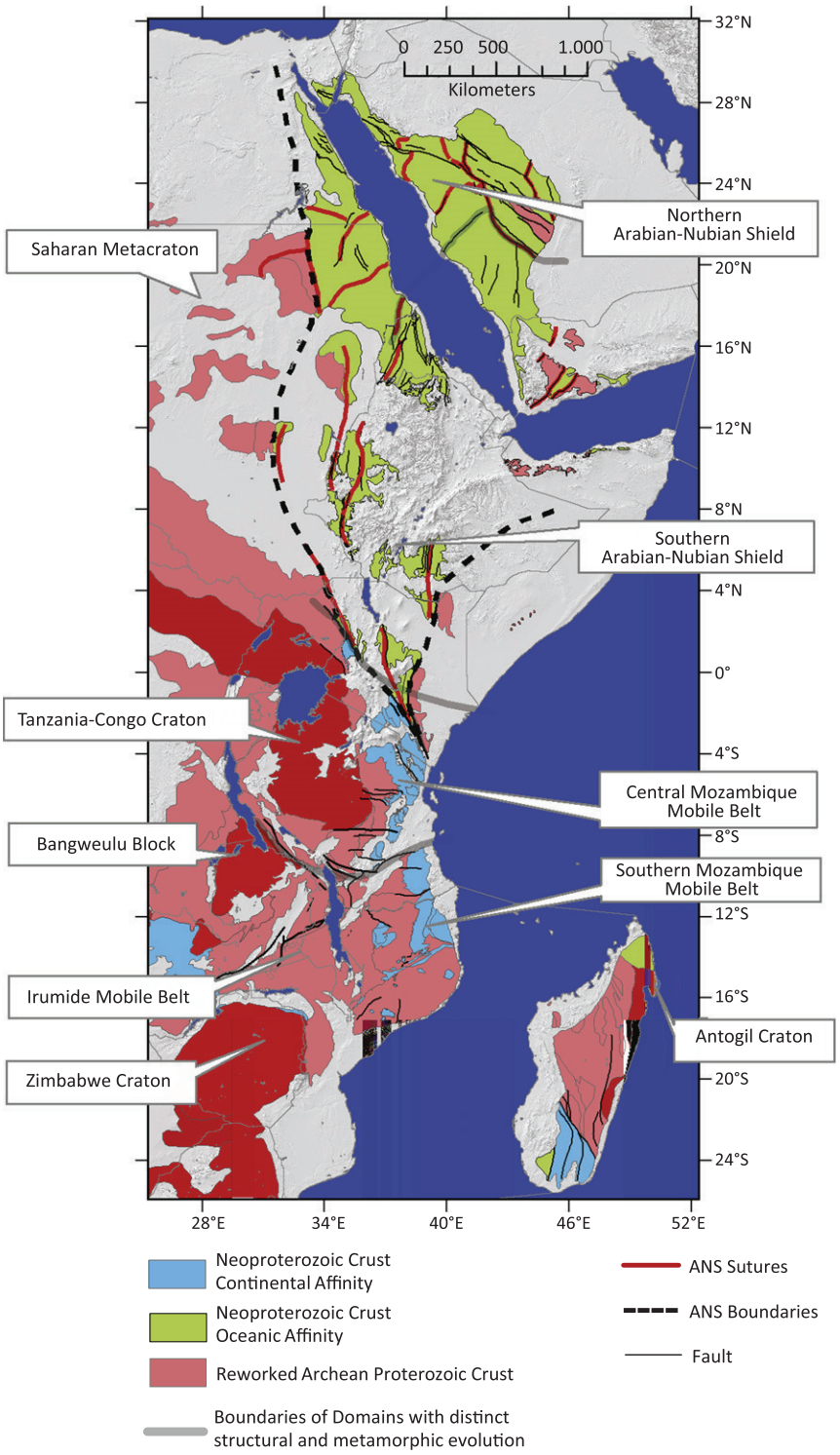

Fig. 2. The Arabian–Nubian Shield in relation to East Africa as component parts of the East African Orogen. Although the Arabian–Nubian Shield extends as far south as southern Kenya, the geographic focus of this review is on the ANS between northern Ethiopia and Sinai and Jordan.

Contemporary Neoproterozoic orogenic belts were present in other parts of greater Gondwana at the end of the Precambrian as the result of similar events of crustal accretion (e.g., Grunow, 1999; Abdelsalam et al., 2003; Collins and Pisarevsky, 2005; Brito Neves and Cordani, 1991).

For the purpose of this review, the margins of the ANS are defined as the limits of Neoproterozoic juvenile rocks of the type exposed on the Shield. The western margin is reasonably well delineated in northern Sudan (Figs. 1 and 2) where >900 Ma biotite–muscovite gneiss, biotite–garnet schist, and mica schist, amphibolite, and hornblende gneiss are overthrust from the north and east by low-grade rocks of ANS affinity belonging to the Atmur–Delgo belt exposed in the Rahaba–Absol terrane (Schandelmeier et al., 1994; Harms et al., 1994; Abdelsalam et al., 1995, 1998, 2002), and by 800–900 Ma high-grade metamorphic rocks in the east (Küster and Liégeois, 2001; Küster et al., 2008).

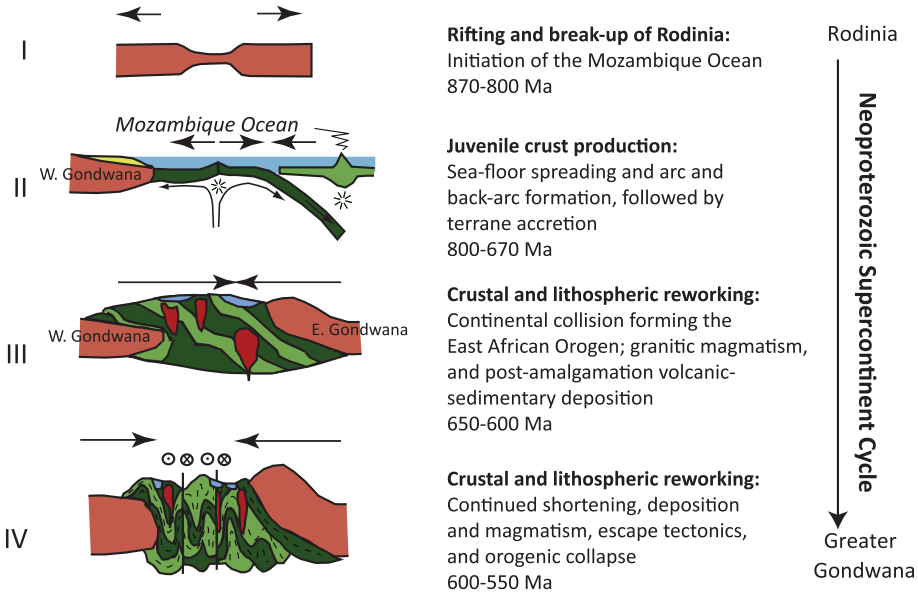

Fig. 3. Schematic illustration of stages in the development of ANS showing its setting in the supercontinent cycle bracketed by the break-up of Rodinia and the assembly of Gondwana. After Stern and Johnson (2010).

Deformation and nappe emplacement along the Atmur–Delgo belt were completed before 700 Ma (Abdelsalam et al., 1995). The Keraf suture, a north-trending belt of deformation at the eastern margin of the Bayuda Desert coincident with the contact between the ANS and the Saharan Metacraton was active between 640 and 560 Ma (Abdelsalam et al., 1998; Bailo et al., 2003). The contact is inferred to extend north into the area immediately west of the Ediacaran granites of Aswan and farther north into the area west of the Eastern Desert of Egypt.

The eastern margin of the ANS is much more ambiguous. Contacts between ~1820 and ~1400 Ma metasedimentary and metaplutonic rocks and younger Neoproterozoic supracrustal deposits (Inda-Ad and Abdulkadir complexes) are exposed in northern Somalia (Kröner and Sassi, 1996), but Neoproterozoic rocks extend across northern Somalia as far as the Indian Ocean and there is no sign of a limit to the ANS. The contact region in Yemen comprises structurally juxtaposed low-grade island-arc Neoproterozoic terranes (Al Bayda and Al Mukalla) and gneissic terranes (Abas and Al Mahfid). The gneissic terranes yield negative initial ε_{Nd} (−5.0 to −39.8), and have late Archean Nd model ages (~2.7–3.0 Ga) and U–Pb ion-microprobe zircon-core ages as old as 2.5 Ga indicating Archean–Paleoproterozoic origins, but were reworked during the Neoproterozoic (Whitehouse et al., 1998, 2001; Windley et al., 1996). The region is interpreted as an alternation of early Precambrian gneissic domains and Neoproterozoic island-arc domains that coalesced to form an arc-gneiss collage contemporaneous with accretionary events in the main part of the ANS.

Paleoproterozoic rocks also crop out in the Khida terrane (Stacey and Agar, 1985; Stoeser and Stacey, 1988; Stoeser et al., 2001), part of the Afif composite terrane, at the eastern margin of the Arabian Shield in Saudi Arabia. The Khida terrane was defined originally on the basis of evolved lead isotopes indicating a component of old continental lead in contrast to juvenile oceanic lead obtained from feldspar and galena samples elsewhere in the Arabian Shield (Stacey et al., 1980; Stoeser and Stacey, 1988) and on the basis of a U–Pb age of 1628 ± 200 Ma (Stacey and Hedge, 1984: Sample Z-103). The age of Z-103 has since been demonstrated to be 750 Ma (Whitehouse et al., 2001), but intact Paleoproterozoic rock has been discovered in adjacent exposures (Whitehouse et al., 2001; Stoeser et al., 2001) and the areal extent of evolved Pb isotopes has been increased (Fig. 4). Most exposed rocks in the Khida terrane are Cryogenian arc assemblages and late Cryogenian to Ediacaran granites, in terms of their crystallization ages, but their negative initial ε_{Nd}, Paleoproterozoic Nd model ages, and evolved Sr and O isotopic signatures (Whitehouse et al., 2001; Stoeser and Frost, 2006) imply the presence of older continental material in the subsurface. Similarities exist between the Khida terrane and the continental terranes in Yemen (Windley et al., 1996; Whitehouse et al., 1998, 2001) and Stoeser and Frost (2006) propose that the Khida terrane is the northwesternmost portion of an "Arabian Craton" underlying the central and southern part of the Arabian Peninsula that was part of the East Gondwana continent. Collins and Pisarevsky (2005) and Raharimahefa and Kusky (2006) treat the same rocks as part of a belt of Archean and Paleoproterozoic crust referred to as "Azania" extending along the eastern margin of the East African Orogen between Madagascar and Arabia. The character of the Arabian Plate basement farther east is uncertain because of Phanerozoic cover as much as 14 km thick. A crustal boundary mapped on the basis of magnetic and gravity data extends north from the Ar Rayn and Ad Dawadimi terranes through central and northern Arabia (Johnson and Stewart, 1995; Sharland et al., 2001; Stern and Johnson, 2010). The crust east of this boundary—the Rayn microplate of Al-Husseini (2000)—contains magnetic highs suggesting the presence of buried arc terranes (Johnson and Stewart, 1995) but the age of the crust and whether it is an extension of the ANS or a crustal block of different provenance are not currently known. Crystalline basement farther east in Oman contains juvenile Neoproterozoic plutonic, metamorphic, and sedimentary rocks similar to those of the ANS, although the timing of magmatism and sedimentation suggests that the Oman crust has a different history to the ANS. Stern and Johnson (2010) reviewed available rock ages and detrital zircons from the Huqf Group to conclude that the crust beneath the Arabian Platform was Cryogenian.

There is evidence from Sinai that ~1 Ga crust flanks the ANS to the north, although actual rock of this age has not yet been identified. Be'eri-Shlevin et al. (2009a) reported abundant 1.0 Ga detrital zircons from Sa'al Group metasedimentary rocks, and concluded that crust of this age must be nearby. Stern et al. (2010a) found that the Zaghra conglomerate contained concordant zircons with

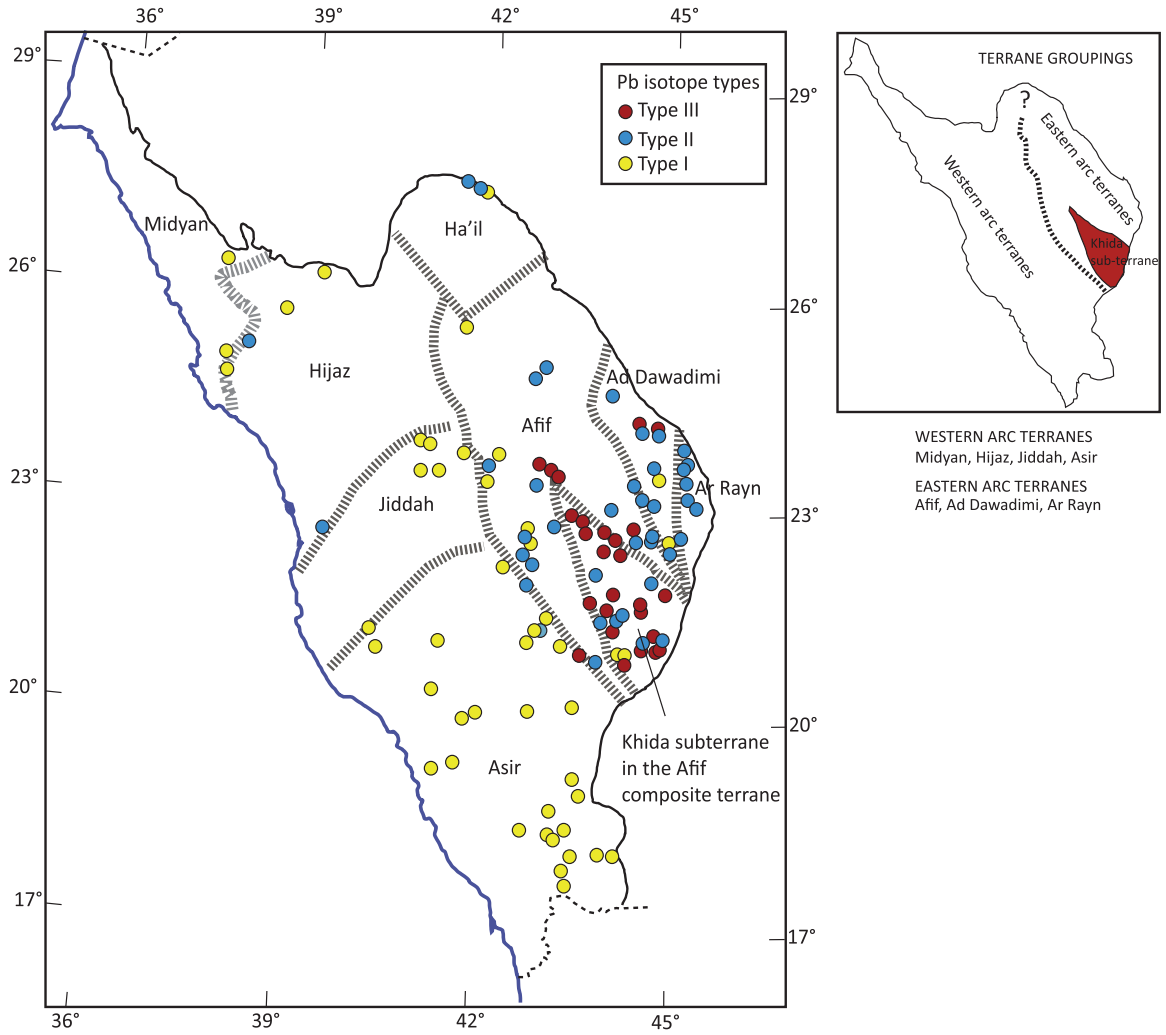

Fig. 4. Distribution of Pb isotope types in the Arabian Shield in Saudi Arabia (after Stoeser and Frost (2006) and Hargrove et al. (2006)), showing a tripartite division of the Arabian Shield into: (1) western intraoceanic juvenile arcs; (2) eastern arcs with continental contributions; and (3) the Khida terrane with highly evolved Pb isotopes indicating a significant contribution from older basement.

two groups of $^{206}Pb/^{238}U$ ages: 931 ± 14 Ma and 606 ± 10 Ma, and plotted a U–Pb discordia for the Zaghra metaconglomerate that has an upper intercept of 1045 ± 55 Ma and lower intercept of 569 ± 55 Ma. Bea et al. (2009), furthermore, found three zircon grains in the 844 Ma Abu Moneiga quartz diorite, located within the Katherine ring-complex in central Sinai, that have inherited cores of 1045 ± 13 Ma, 1046 ± 13 Ma, and 1025 ± 13 Ma, implying that the magmatic source of the Moneiga quartz-diorites involved ~1045 Ma to ~1025 Ma rocks. In this context it is interesting that Nd–Sr–Hf–O isotope data confirm that early crustal evolution in Sinai involved some crustal contamination by pre-ANS material (Be'eri-Shlevin et al., 2010). Isotopic provinciality is shown by post-collisional calc-alkaline and alkaline igneous rocks for ~635–570 Ma across Sinai, with silicic rocks in the northwest having lower $\varepsilon_{Nd}(T)$–$\varepsilon_{Hf}(T)$ and higher Sr_i and $\delta^{18}O$ than those to the southwest.

1.2. Pre-650 Ma arc-magmatism and terranes

Most pre-650 Ma rocks in the ANS are parts of Tonian–middle Cryogenian island-arc terranes (Fig. 5A) that developed in the Mozambique Ocean between rifted blocks of the Rodinia supercontinent and other cratons (Stoeser and Camp, 1985; Genna et al., 2002; Johnson and Woldehaimanot, 2003; Stoeser and Frost, 2006). They typically have crystallization ages close to their Nd model ages, and constitute juvenile additions to the crust (Stern, 2002). The terranes converged and amalgamated as a result of intraoceanic subduction-driven arc–arc and ultimately arc–continent collisions. Most terrane boundaries are high-strain shear zones that commonly contain dismembered ophiolites (Berhe, 1990) and refolded recumbent folds. The shear zones are widely interpreted as sutures that formed at the time of terrane amalgamation, although identification of the shears zones as sutures has been challenged (Church, 1991) and some shear zones are younger strike-slip shear zones that modified or reworked original sutures (e.g., Kusky and Matsah, 2003).

The oldest Neoproterozoic crust is in the Tokar/Barka–Asir terrane (the hyphen here indicating correlation across the Red Sea), the Jiddah–Haya terrane, and the Hijaz–Gebeit terrane. Although the crust in Eritrea is divided by many workers into many individually named domains (Drury and De Souza Filho, 1998), the composite term "Tokar/Barka terrane" is used here for convenience. The terranes converged and amalgamated during the middle Cryogenian along the Barka and Bir' Umq–Nakasib sutures (780–750 Ma) (Fig. 5B), resulting in a core grouping of terranes. By 700 Ma, the Midyan–Eastern Desert terrane had collided and amalgamated with the core group of terranes along the Yanbu and Sol Hamid–Allaqi–Heiani sutures, comprising a geologic entity

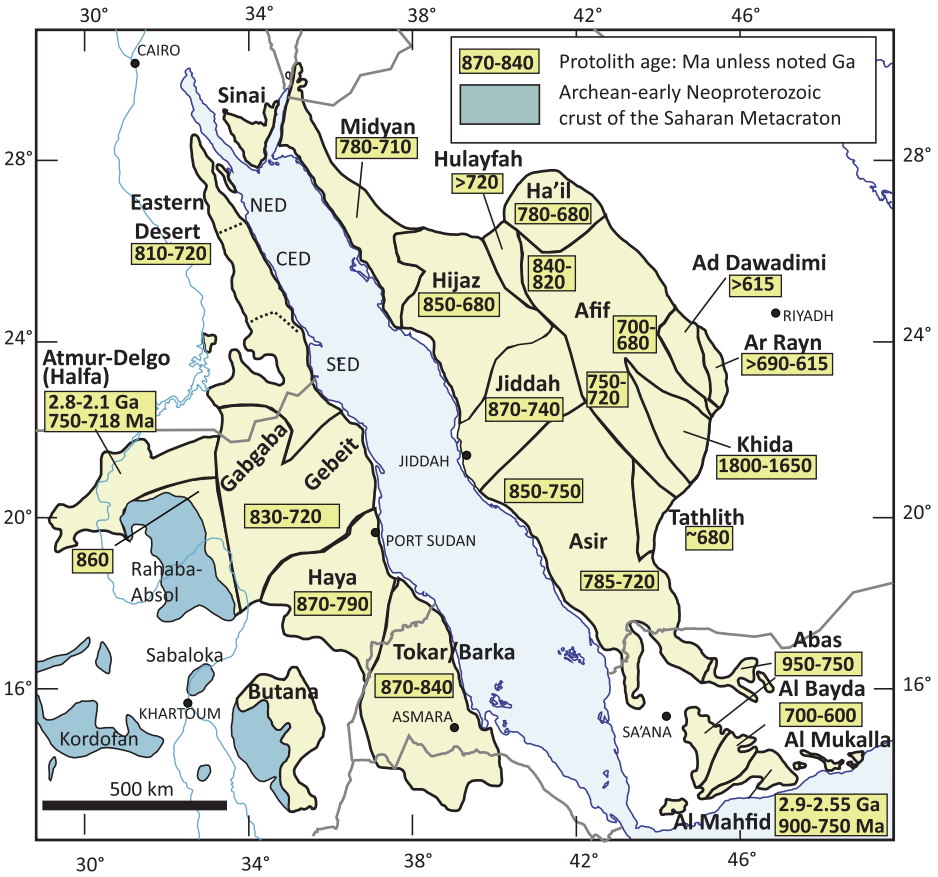

Fig. 5A. ANS tectonostratigraphic terranes, showing protolith ages. NED = North Eastern Desert; CED = Central Eastern Desert; SED = Southern Eastern Desert.

commonly referred to as the "western arc or oceanic terranes" of the ANS (e.g., Stoeser and Frost, 2006).

The Sol Hamid–Allaqi–Heiani suture (Stern et al., 1989; Stern, 1994; Abdelsalam and Stern, 1996) separates the South Eastern Desert (SED) (Gerf) terrane on the north (Kröner et al., 1987; Greiling et al., 1994; Shackleton, 1994; Abdelsalam and Stern, 1996; Kusky and Ramadan, 2002) from the 830–700 Ma Gebeit and Gabgaga terranes on the south. It strikes roughly east, but swings to the south in its middle section as it merges with and is overprinted by the NNE-trending Hamisana shear zone (de Wall et al., 2001). Relatively high-grade gneissic rocks of the SED terrane are interpreted as island-arc and ophiolitic nappes uplifted as they were thrust south over the Gebeit and Gabgaba terranes (Greiling et al., 1994; Kusky and Ramadan, 2002). The Gabgaba terrane contains an island arc assemblage (El-Nisr, 1997), including metavolcanic rocks and bands of marble, interpreted as deformed shallow-water carbonates that originally fringed the arc volcanics (Greiling et al., 1994).

The core group of ANS terranes subsequently collided and amalgamated between about 680 Ma and 640 Ma with the Afif and Tathlith terranes, creating a neocontinental crustal block referred to here as the proto-Arabian–Nubian Shield (pANS). The 680–640 Ma assembly of the pANS was associated with metamorphic, deformational, and intrusive events that, in the Arabian Shield, are referred to as the "Nabitah orogeny" (680–640 Ma) (Stoeser and Stacey, 1988). The orogeny is named after the Nabitah fault, the suture between the Asir and Tathlith terranes and a ductile shear zone within the Asir terrane. The fault gives its name to the Nabitah mobile belt (Stoeser and Stacey, 1988) (Fig. 5B), a broad zone of deformation and metamorphism that trends N–S across the Arabian Shield. The mobile belt encompasses the suture between the Afif terrane and western oceanic terranes and the suture between the Asir and Tathlith terranes. The Afif terrane is a composite tectonostratigraphic unit comprising the Paleoproterozoic Khida terrane (or subterrane) and three Neoproterozoic arc assemblages of about 840–820 Ma, 750–720 Ma, and 700–680 Ma (Fig. 5A). The Afif terrane and the western oceanic terranes were fully amalgamated by about 640 Ma. The youngest terranes in the ANS, with upper Cryogenian to Ediacaran protoliths, are the Ad Dawadimi and Ar Rayn terranes in the easternmost Arabian Shield. The history of these terranes is not fully established but is critical to our understanding of the tectonic evolution of the ANS (Cox et al., 2011) and is further described below. A suturing event along the eastern margin of the Afif terrane is marked by formation of the Halaban ophiolite at ~680–670 Ma (Al-Saleh et al., 1998). However, deposition of the Abt group, which makes up most of the Ad Dawadimi terrane, continued until ~620 Ma, when it was metamorphosed to greenschist and lower amphibolite facies (Cox et al., 2011) and when the Ad Dawadimi and Ar Rayn terranes amalgamated with the western oceanic terranes. This event was broadly contemporary with accretion of the entire ANS to the East Saharan craton along the arc–continent Keraf suture (~650–560 Ma) (Abdelsalam et al., 1998; Bailo et al., 2003), a sinistral transpressional suturing event that was one of the principal tectonic elements in the final assembly of Gondwana. The accretion of the ANS to the Saharan Metacraton is analogous to the proposed ~650–630 Ma collision of Azania with the East African margin in the southern Mozambique Belt (Collins and Windley, 2002; Collins and Pisarevsky, 2005; Collins, 2006; Collins et al., 2010). Collins and

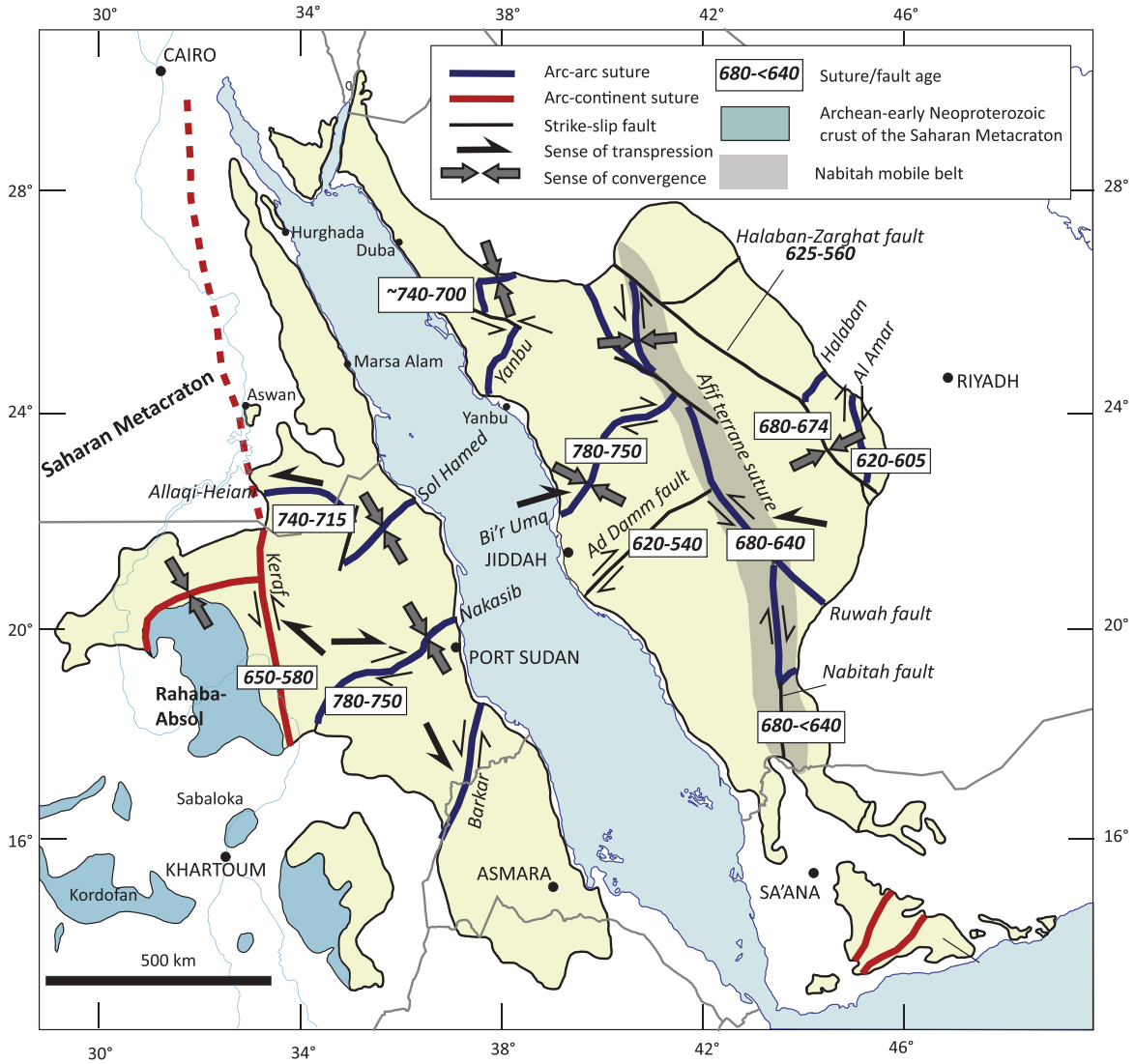

Fig. 5B. Terrane assembly in the ANS showing inferred ages of suturing and fault movements, and trajectories of amalgamation.

Pisarevsky (2005) suggested that the term the "East African Orogeny" be restricted to this event.

Terranes in the southern part of the ANS are widely disrupted by north-trending shears and shortening zones (Abdelsalam and Stern, 1996). Farther north, terranes are disrupted by northwest-trending shears belonging to the Najd fault system, although the amount of displacement and extent of deformation associated with the Najd system is controversial (e.g., Sultan et al., 1988; Andre, 1989; Sengör and Natalin, 1996; Smith et al., 1998; Kusky and Matsah, 2000, 2003; Johnson et al., 2004).

2. Late Cryogenian–Ediacaran geochronologic data base

The timing of 650–542 Ma events in the ANS is constrained by an extensive U–Pb, Pb–Pb, Rb–Sr, and Sm–Nd geochronologic database (Appendix A). The locations of the samples dated are plotted on Fig. 6. There are, of course, many age dates in the ANS for the period >650 Ma, but they are not shown on this figure because they are outside the time frame of our review (see Johnson and Kattan, 2007 for data about the Arabian Penninsula and Stern et al., 2010b for information about U–Pb and Pb–Pb ages in both the Arabian and Nubian Shields). $^{40}Ar/^{39}Ar$ measurements are not as numerous, but the results provide important constraints on metamorphic and exhumation events; they are separately listed in Table 1.

A frequency histogram of robust crystallization ages (Fig. 7A) shows peaks suggesting surges in magmatic activity in the ANS at 635 Ma, 610 Ma, 600 Ma, and 580 Ma. Bias must be taken into account when interpreting this histogram since most geochronologic data in the ANS have been obtained from granitoids, and somewhat different plots result from dividing the data according to broad rock type (Fig. 7B–E). Extrusive volcanic rocks in the ANS are commonly difficult to date because they yield fewer zircons than intrusive rocks: in addition, they contain more xenocrystic zircons (Stern et al., 2010b). As a consequence, ANS volcanic events are not as well constrained as intrusive events.

The growing number of ion microprobe zircon ages in the ANS has revealed that a small, but significant, number of ANS igneous rocks contain zircons that are significantly older than the crystallization ages of the host rocks (Küster et al., 2008; Be'eri-Shlevin et al., 2009c; Stern et al., 2010b). Inheritance in the Arabian Shield was first indicated by a report of zircons dating 1986 ± 200 Ma (Calvez et al., 1985) in Neoproterozoic plagiogranite immediately west of the Al Amar fault. A recent compilation (Stern et al., 2010b) shows that about 5% of individually dated zircons from ANS Neoproterozoic igneous rocks have ages older than 880 Ma,

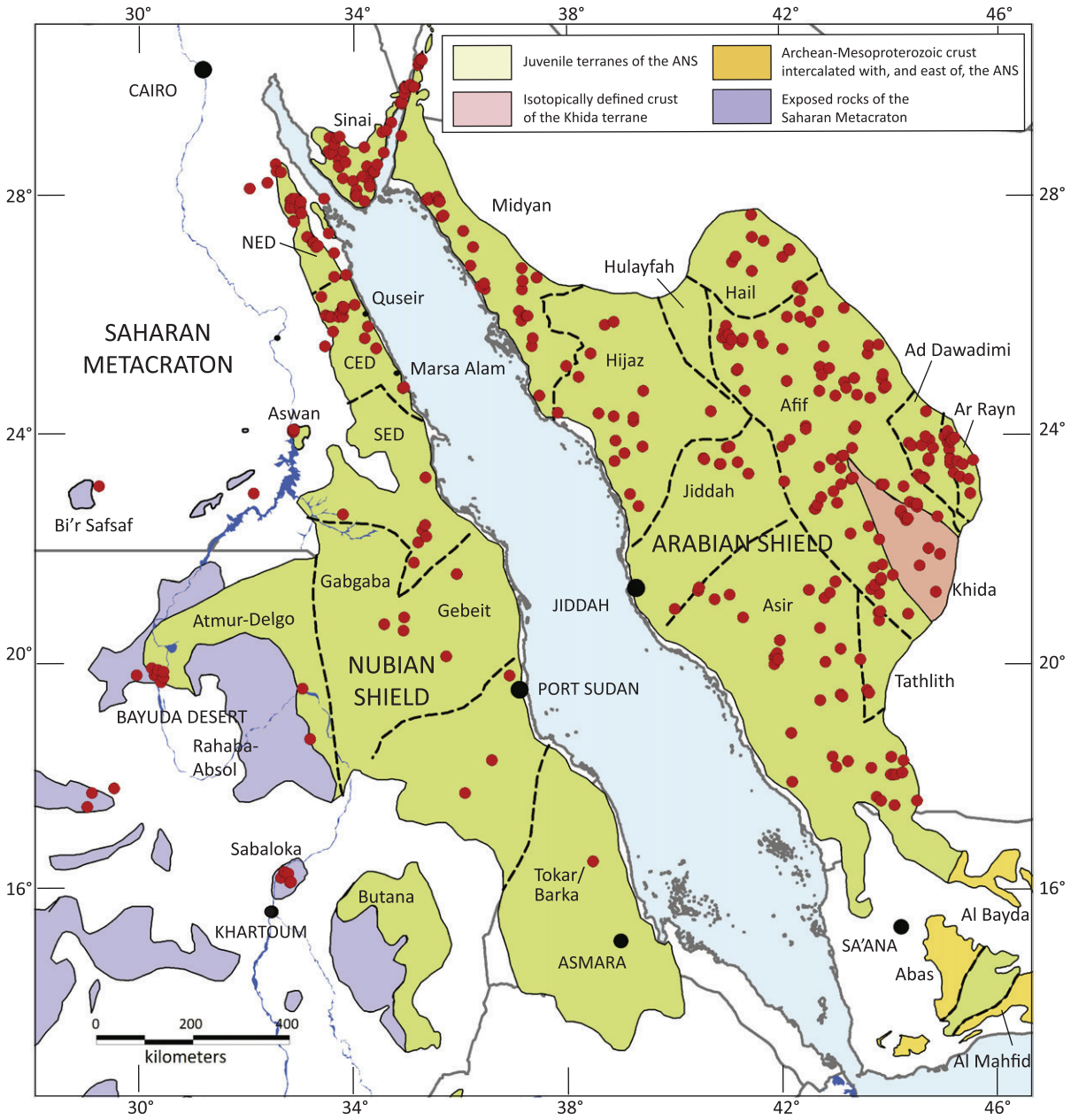

Fig. 6. Map of the Arabian–Nubian Shield showing the locations of rock samples with late Cryogenian–Ediacaran U–Pb, Sm–Nd, and Rb–Sr ages in the range 650–542 Ma. Details of the samples are given in Appendix A.

with concentrations in the Tonian–Mesoproterozoic (0.9–1.15 Ga); late Paleoproterozoic (1.7–2.1 Ga); Paleoproterozoic–Neoarchean (2.4–2.8 Ga); and early Archean (>3.2 Ga). Explanations for inheritance include: (1) contamination during processing; (2) assimilation from cryptic early Neoproterozoic to Archean basement; (3) assimilation of terrigenous sediment shed from nearby passive margins transported by rivers or glaciers; and (4) inheritance from a mantle source (Stern et al., 2010b).

3. Post-amalgamation basins

Deposition in the ANS prior to 650 Ma was dominated by volcanosedimentary assemblages in volcanic arcs; after 650 Ma, deposition changed to volcanosedimentary assemblages in post-amalgamation basins overlying newly amalgamated arc terranes. In contrast to the arc assemblages, the post-amalgamation-basin successions have unconformable basal contacts, indicating that they are autochthonous, in place at their site of deposition. The basal contacts vary from angular unconformities to nonconformities, in places grading from *in situ* weathered rubble on plutonic substrates up into conglomerate, sandstone, and siltstone. The post-amalgamation deposits occur throughout the ANS, but are mostly developed in the north and northeast (Figs. 8 and 9). Some deposits are as old as 660–650 Ma, but most are late Cryogenian to Ediacaran (Table 2). The basin deposits are variably deformed with gentle to vertical dips, and open-to-tight folds. Cleavage and lineations are common and some deposits are affected by ductile shearing and mylonitization. Most deposits are only weakly to moderately metamorphosed, apart from exceptions such as the Atura formation (<650 to >640 Ma), in the southern part of the Arabian Shield, which is at amphibolite grade (Fairer, 1985). The basins vary in

Table 1
Late Cryogenian–Ediacaran $^{40}Ar/^{39}Ar$ age dates from the Arabian–Nubian shield.

Sample	Plateau age	Isochron age	Laser fusion	Geologic unit	Lithology	Mineral dated	MSWD	Comment	Reference
Sibai 6	623.6 ± 0.2			Abu Markhat gneiss, Sibai dome	Hornblende-rich gneiss	Horblende		Interpreted as cooling below 500 °C; protolith age ~645 Ma	Fritz et al. (2002)
Ar-24	616 ± 3	625 ± 88	799	Shahmon Metabasite	Undeformed gabbro	Amphibolite		Disturbed $^{40}Ar/^{39}Ar$ spectra	Cosca et al. (1999)
S08-17	616 ± 2.8	617.52 ± 5.25		Metasedimentary siltstone (Abt formation)	Biotite–muscovite–chlorite schist	Muscovite	0.63	Interpreted as metamorphic muscovite with result giving the age of metamorphism	Lewis (2009)
S08-15	613 ± 5.9 618 ± 6*	615.51 ± 6.42 621 ± 4*		Metasedimentary siltstone (Abt formation)	Biotite–muscovite–chlorite schist	Muscovite	1.6	Interpreted as metamorphic muscovite with result giving the age of metamorphism. * = ages recalculate using decay constants revised by Renne et al., 2010	Lewis (2009)
RD-3	612 ± 3	612 ± 2		Ar Ridaniyah ophiolite melange	Metagabbro	Hornblende	0.8	Records time of cooling below blocking temperature of hornblende. Interpreted as 'uplift age' evidencing Ediacaran tectonic activity associated with rejuvenation of Ar Ridaniyah thrust fault after obduction of ophiolite 60 Ma earlier	Al-Saleh and Boyle (2001)
RD-9	611 ± 8	617 ± 6		Ar Ridaniyah ophiolite melange	Metagabbro	Hornblende	11.7	Records time of cooling below blocking temperature of hornblende. Interpreted as 'uplift age' evidencing Ediacaran tectonic activity associated with rejuvenation of Ar Ridaniyah thrust fault after obduction of ophiolite 60 Ma earlier	Al-Saleh and Boyle (2001)
RD-2	610 ± 2	612 ± 2		Ar Ridaniyah ophiolite melange	Amphibolite	Hornblende	0.5	Records time of cooling below blocking temperature of hornblende. Interpreted as 'uplift age' evidencing Ediacaran tectonic activity associated with rejuvenation of Ar Ridaniyah thrust fault after obduction of ophiolite 60 Ma earlier	Al-Saleh and Boyle (2001)
AD 24-25.4	609 ± 1.3		611 ± 1	Ad Duwayhi gold-bearing quartz vein	Quartz veins	Sericite		Inferred to be age of a post-mineralization thermal event, perhaps associated with late intrusions in the Haml batholith	Doebrich et al. (2004)
Sibai 5	606.7 ± 0.2			Pre-intrusive amphibolitic lens, Sibai dome	Amphibolitic lens	Hornblende		Interpreted as a possible second phase of cooling ~ 20 million years after onset of cooling (623 Ma) associated with denudation or cooling after advecive heating by granitoid intrusion	Fritz et al. (2002)
AD24-81.6	603 ± 1		608 ± 1	Ad Duwayhi gold-bearing quartz vein	Quartz veins	Sericite		Inferred to be age of a post-mineralization thermal event, perhaps associated with late intrusions in the Haml batholith	Doebrich et al. (2004)
Ar-12	601.4 ± 2.0		594	Taba tonalite gneiss		Biotite		Interpreted as age of regional metamorphic cooling, not a resetting event	Cosca et al. (1999)
HF 50	601 ± 4	599 ± 3		At Tari Structural Window	Migmatite	Hornblende		Closeness of both biotite and hornblende ages from the At Tari window suggst rapid uplift and cooling of the window	Al-Saleh et al. (1998)
Ar-31	598.4 ± 1.4		599	Elat Schist	Garnetiferous leucosome	Muscovite		Muscovite obtained from a late granitoid dike in Elat Schist. Interpreted as age of regional metamorphic cooling, not a resetting event	Cosca et al. (1999)
HC-60	597 ± 4	601 ± 5		Halaban sub-ophiolite complex	Amphibolite	Hornblende		Perhaps reset during emplacement of Abu Isnun pluton	Al-Saleh et al. (1998)
HF 54	597 ± 2	598 ± 3		At Tari Structural Window	Garnet–biotite schist	Biotite		Closeness of both biotite and hornblende ages from the At Tari window suggst rapid uplift and cooling of the window	Al-Saleh et al. (1998)
Ar-18	597.0 ± 1.4		597	Elat granite	Undeformed late- to post-kinematic granite	Biotite		Interpreted as age of regional metamorphic cooling, not a resetting event	Cosca et al. (1999)
RD-7	596 ± 6	602 ± 2		Ar Ridaniyah ophiolite melange	Metagabbro	Hornblende	1.5	Records time of cooling below blocking temperature of hornblende. Interpreted as 'uplift age' evidencing Ediacaran tectonic activity associated with rejuvenation of Ar Ridaniyah thrust fault after obduction of ophiolite 60 Ma earlier	Al-Saleh and Boyle (2001)
Meatiq 2	595.9 ± 0.5			Meatiq dome, southern low-angle normal fault	Shear-zone rock	Muscovite		Metamorphic age of muscovite forming at expense of feldspar during shearing; is similar to cooling ages and is consistent with interpretation that exhumation within the Meatiq dome was contemporary with shearing and extension on the margins	Fritz et al. (1996)
E98	594 ± 6			Ghedem terrane mylonitized gneiss	Titanite–amphibole gneiss and amphibolite	Hornblende		Cooling age after peak metamorphism at about 593 Ma; time of exhumation associated with orogenic collapse	Ghebreab et al. (2005)
Ar-16	592 ± 4	591 ± 9	575	Elat granite gneiss		Biotite		Interpreted as age of regional metamorphic cooling, not a resetting event	Cosca et al. (1999)
Meatiq 1	588.2 ± 0.3			Meatiq dome, western shear zone	Shear-zone rock	Muscovite		Metamorphic age of muscovite forming at expense of feldspar during shearing; is similar to cooling ages and is consistent with	Fritz et al. (1996)

						interpretation that exhumation within the Meatiq dome was contemporary with shearing and extension on the margins	
Meati2 2	587.3 ± 0.2			Um Baanib gneiss, Meatiq Dome	Amphibolitic schollen	Hornblende	Interpreted as post-metamorphic cooling below 500 °C. Age is similar to that of muscovite (582 Ma) suggesting rapid cooling and exhumation	Fritz et al. (2002)
G2A	586 ± 6			Ghedem terrane mylonitized gneiss	Titanite–amphibole gneiss and amphibolite	Hornblende	Cooling age after peak metamorphism at about 593 Ma; time of exhumation associated with orogenic collapse	Ghebreab et al. (2005)
Hafafit 7	586.1 ± 0.3			Orthogneiss, Hafafit dome	Orthogneiss	Hornblende	Interpreted as cooling age below 500 °C associated with exhumation of Hafafit dome along NE-trending extensional faults. Protolith ages of granitoid gneiss are 682 Ma, 689 Ma, and 700 Ma	Fritz et al. (2002)
Hafafit 8	584.2 ± 0.2			Orthogneiss, Hafafit dome	Orthogneiss	Hornblende	Interpreted as cooling age below 500 °C associated with exhumation of Hafafit dome along NE-trending extensional faults. Protolith ages of granitoid gneiss are 682 Ma, 689 Ma, and 700 Ma	Fritz et al. (2002)
E99	583 ± 5			Ghedem terrane mylonitized gneiss	Titanite–amphibole gneiss and amphibolite	Hornblende	Cooling age after peak metamorphism at about 593 Ma; time of exhumation associated with orogenic collapse	Ghebreab et al. (2005)
Meatiq 4	583.9 ± 0.2			Um Baanib gneiss, Meatiq Dome	Amphibolitic schollen	Hornblende	Interpreted as post-metamorphic cooling below 500 °C. Age is similar to that of muscovite (582 Ma) suggesting rapid cooling and exhumation	Fritz et al. (2002)
Meatiq 9	582.3 ± 0.2			Garnet kyanite schist, Meatiq dome	Garnet–kyanite schist	Muscovite	Interpreted as cooling below ~375–400 °C (blocking temperature for muscovite). Result is similar to that for hornblende (587–579 Ma) suggesting rapid cooling and exhumation	Fritz et al. (2002)
Meatiq 1	580.3 ± 0.3			Um Baanib gneiss, Meatiq Dome	Amphibolitic schollen	Hornblende	Interpreted as post-metamorphic cooling below 500 °C. Age is similar to that of muscovite (582 Ma) suggesting rapid cooling and exhumation	Fritz et al. (2002)
E9B	579 ± 5			Ghedem terrane mylonitized gneiss	Titanite–amphibole gneiss and amphibolite	Hornblende	Cooling age after peak metamorphism at about 593 Ma; time of exhumation associated with orogenic collapse	Ghebreab et al. (2005)
Meatiq 3	579.1 ± 0.2			Um Baanib gneiss, Meatiq Dome	Amphibolitic schollen	Hornblende	Interpreted as post-metamorphic cooling below 500 °C. Age is similar to that of muscovite (582 Ma) suggesting rapid cooling and exhumation	Fritz et al. (2002)
K95-5-3	577 ± 5			Granite: Abu Hamed shear zone	Highly deformed granite	Biotite	Cooling age; dates cessation of ductile deformation on Abu Hamed shear zone and sinistral transpression on Keraf suture at ~577 Ma	Abdelsalam et al. (1998)
K95-5-3	577 ± 2			Granite: Abu Hamed shear zone	Highly deformed granite	Biotite	Cooling age; dates cessation of ductile deformation on Abu Hamed shear zone and sinistral transpression on Keraf suture at ~577 Ma	Abdelsalam et al. (1998)
K95-5-3	577 ± 2			Granite: Abu Hamed shear zone	Highly deformed granite	Hornblende	Cooling age; dates cessation of ductile deformation on Abu Hamed shear zone and sinistral transpression on Keraf suture at ~577 Ma	Abdelsalam et al. (1998)
G26	576 ± 6			Ghedem terrane mylonitized gneiss	Quartz-feldspar gneiss	Muscovite	Cooling age after peak metamorphism at about 593 Ma; time of exhumation associated with orogenic collapse	Ghebreab et al. (2005)
E9A	572 ± 7			Ghedem terrane mylonitized gneiss	Titanite–amphibole gneiss and amphibolite	Hornblende	Cooling age after peak metamorphism at about 593 Ma; time of exhumation associated with orogenic collapse	Ghebreab et al. (2005)
G26H	572 ± 6			Ghedem terrane mylonitized gneiss	Titanite–amphibole gneiss and amphibolite	Hornblende	Cooling age after peak metamorphism at about 593 Ma; time of exhumation associated with orogenic collapse	Ghebreab et al. (2005)
E97	566 ± 5			Ghedem terrane mylonitized gneiss	Quartz-feldspar gneiss	Muscovite	Cooling age after peak metamorphism at about 593 Ma; time of exhumation associated with orogenic collapse	Ghebreab et al. (2005)
G2C	565 ± 7			Ghedem terrane mylonitized gneiss	Titanite–amphibole gneiss and amphibolite	Hornblende	Cooling age after peak metamorphism at about 593 Ma; time of exhumation associated with orogenic collapse	Ghebreab et al. (2005)
E27	564 ± 5			Ghedem terrane mylonitized gneiss	Quartz-feldspar gneiss	Muscovite	Cooling age after peak metamorphism at about 593 Ma; time of exhumation associated with orogenic collapse	Ghebreab et al. (2005)
E2B	563 ± 5			Ghedem terrane mylonitized gneiss	Quartz-feldspar gneiss	Muscovite	Cooling age after peak metamorphism at about 593 Ma; time of exhumation associated with orogenic collapse	Ghebreab et al. (2005)
Ar-16			607	Elat granite gneiss		Biotite	Interpreted as age of regional metamorphic cooling, not a resetting event	Cosca et al. (1999)
AR-24			595	Shahmon Metabasite	Undeformed gabbro	Phlogopite	Interpreted as age of regional metamorphic cooling, not a resetting event	Cosca et al. (1999)
K-1		557 ± 15		Kirsh gneiss belt	Biotite paragneiss	Biotite	Interpreted as cooling age and minimum age of development of Kirsh gneiss belt. Broadly coeval with Rb–Sr w.r. isochron of 535 Ma and K–Ar hornblende age of 588 Ma for foliated granitoid between Ruwah and Ar Rika fault zones	Al-Saleh (2010)

surface area from as much as about 72,000 km^2 for the largest, the Murdama basin in the northeastern ANS, to small isolated basins of 200 km^2 (e.g., Johnson, 2003; Matsah and Kusky, 1999, 2001; Willis et al., 1988; Abdeen and Greiling, 2005; Eliwa et al., 2006, 2010). The deposits may be entirely or largely volcanic or volcaniclastic in origin; many include volcanic, volcaniclastic, and epiclastic rocks; others are dominantly or entirely sedimentary. The depositional environments range from terrestrial to shallow marine and include scarp front and alluvial settings as well as marine basins or basins connected to an ocean. Rocks deposited in terrestrial settings are characterized by red–maroon coloration stained by ferric iron and, in some cases, show rain-prints or mudcracks (Abdeen et al., 1997). Marine settings are indicated by a prevalent gray–green coloration of epiclastic rocks, and the presence of limestone formations up to several hundred meters thick, containing stromatolitic bioherms, undulose algal bedding, suspect multicellular organisms, and isotopes of marine affinity. The evolution of isotopic systems in ancient sedimentary rocks is now well established for the Neoproterozoic (Halverson et al., 2010) and conspicuous perturbations are recognized during the Cryogenian and Ediacaran that are linked with the concept of Snowball Earth and periodic glaciations. The world's largest δC excursion is recorded in Ediacaran sediments in Oman associated with the ~630 Ma Marinoan glaciation (Le Guerroué et al., 2006). A similar, but less extreme, negative anomaly has recently been recorded in the Antaq Basin (Nettle, 2009), but no isotopic evidence of glaciation has been found in any other post-amalgamation basin in the ANS. However, diamictite in some of the Jibalah group basins (Miller et al., 2008) suggests that further evidence may be forthcoming.

Marine post-amalgamation basins, typified by the Murdama, Bani Ghayy, Fatima, and Ablah groups, are prominent in the eastern part of the ANS. They began to be deposited during and soon after the Nabitah orogeny (680–640 Ma) that marked suturing of the Afif terrane with oceanic ANS terranes to the west. The Murdama basin, the largest in the ANS, was deposited on the eastern flank of the Nabitah mobile belt and appears to be a foreland basin. The Bani Ghayy group, similar in age to the Murdama, was deposited in extensional rift basins closer to the axis of the Nabitah mobile belt. The Fatima and Ablah groups were deposited west of the axis of the Nabitah mobile belt. *Terrestrial basins* are chiefly located in the northwestern part of the ANS, in the northern Arabian Shield, in Sinai, and in the Eastern Desert. Small basins occur in Sudan (Amaki formation) at the contact between the ANS and Saharan Metacraton. They include foreland basins, intermontane molasse basins, and strike-slip pull-apart basins not connected to any ocean. Conglomerate is abundant, limestone lacking, and volcanic assemblages extensive. *Mixed terrestrial–shallow marine basins* are present throughout the northern part of the ANS. They contain clastic rocks indicative of subaerial deposition, limestone of marine or possible marine origin, and varying amounts of volcanic rocks. Diamictite and possible dropstones suggest deposition coincident with glaciation. The basins are characterized by the Jibalah group (~590–560 Ma) and appear to have a more restricted time frame than other types of post-amalgamation basins in the ANS.

Despite their abundance and, locally, great thickness, relatively little is known about the development and depositional environments of the post-amalgamation basin in the ANS. Fundamental unanswered questions concern (1) the causes of subsidence that created the basins, whether thermal contraction, loading or flexure downwarping, or extension and pull-apart development in strike-slip systems; (2) the apparent genetic relationships between basin formation and local and regional structures such as strike-slip faulting and mantle doming; (3) the relationship between basin formation and granitoid magmatism; (4) the extent to which some of the basins were originally interconnected; (5) which basins were marine or connected to a late Cryogenian–Ediacaran ocean; and (6) whether any basins contain unequivocal Ediacaran multicellular fossils.

The sedimentary formations in many of the post-amalgamation basins in the ANS are referred to as "molasse" (e.g. Shalaby et al., 2006; Abd El-Wahed, 2009; Genna et al., 2002), implying deposition in front of a rising mountain belt synchronous with orogeny or in intermontane basins in the internal part of a mountain belt as it collapsed and underwent extensional and strike-slip faulting. The abundance of post-amalgamation basins, and the presence of marine deposits in some, implies that large areas of the ANS were depressed during the late Cryogenian and Ediacaran so as to accommodate thick sequences of sedimentary and volcanic rocks and significant parts were below sea level. It is pertinent to question therefore whether the EAO during its formation was a continuous or discontinuous, broken-up mountain belt, whether it was high above sea level and far from oceanic influences, or whether it was deeply penetrated by seaways along valleys and depressions.

3.1. Marine basins

The *Murdama basin* is the largest post-amalgamation basin in the ANS, more than 600 km long and 120 km wide. It crops out at the eastern margin of the Afif terrane and beneath Phanerozoic cover to the southeast (Johnson, 2003). The basin contains the Afif formation, a thin volcanic unit of calc-alkaline to alkaline rhyolite, dacite, andesite, and basalt at the base in the west, and the Murdama group, a thick sandstone, conglomerate, limestone, and subordinate volcanic succession above. In the east, the Murdama group unconformably overlies greenschist- to amphibolite- and, locally, granulite-facies metavolcanic and plutonic rocks of the Afif terrane, a relationship that suggests as much as 15–20 km uplift and erosion prior to Murdama deposition.

The Murdama group is estimated to have been deposited between ~650 and 620 Ma, toward the end of and after the 680–640 Ma Nabitah orogeny. It is dated by U–Pb SHRIMP ages of 630–624 Ma obtained from rhyolite in the southern part of the basin (Kennedy et al., 2010) and by a conventional U–Pb zircon age of 625 ± 4 Ma obtained from volcanic rocks to the northwest (Kusky and Matsah, 2003); in the north, the group may be as old as 650 Ma (Cole and Hedge, 1986). The group is intruded by ~650–570 Ma granitoid plutons (Cole and Hedge, 1986), and by ~630 Ma rhyolite sills (Kennedy et al., 2004).

The Murdama group is dominantly well-bedded fine- to medium-grained gray–green lithic (volcanic) arenite and arkosic arenite, with planar cross bedding, ripple cross lamination, planar lamination, grading, and scour-and-fill features. Upward-fining cycles of sandstone, siltstone, and shale less than 1 to several meters thick are locally present (Wallace, 1986). Polymict conglomerate, in part filling channels, is common at the base of the Murdama group and higher in the sequence. Limestone units, 10 to more than 1000 m thick and commonly stromatolitic, crop out at the base of the group along the eastern margin of the basin. An overall marine environment is clearly identified by the limestone, but in detail the basin appears to grade from a volcanic–plutonic terrain in the west to a marine and shallow-marine basin in the east. Deltaic environments are suggested by Greene (1993) and Cole (1988), whereas Wallace (1986) describes a near-shore mud-flat and broad-channel environment with lagoonal, lacustrine, or shallow-marine carbonate mud and algal buildups in the northern part of the basin. Gently plunging, open, upright, north-trending folds with locally vertical limbs are pervasive, indicating bulk E–W shortening, in part associated with sinistral shearing on transcurrent Najd faults (Moore, 1979; Johnson, 2003).

Smaller marine basins are represented by the Bani Ghayy and Fatima groups. The Bani Ghayy group, about 6000 m thick (Agar,

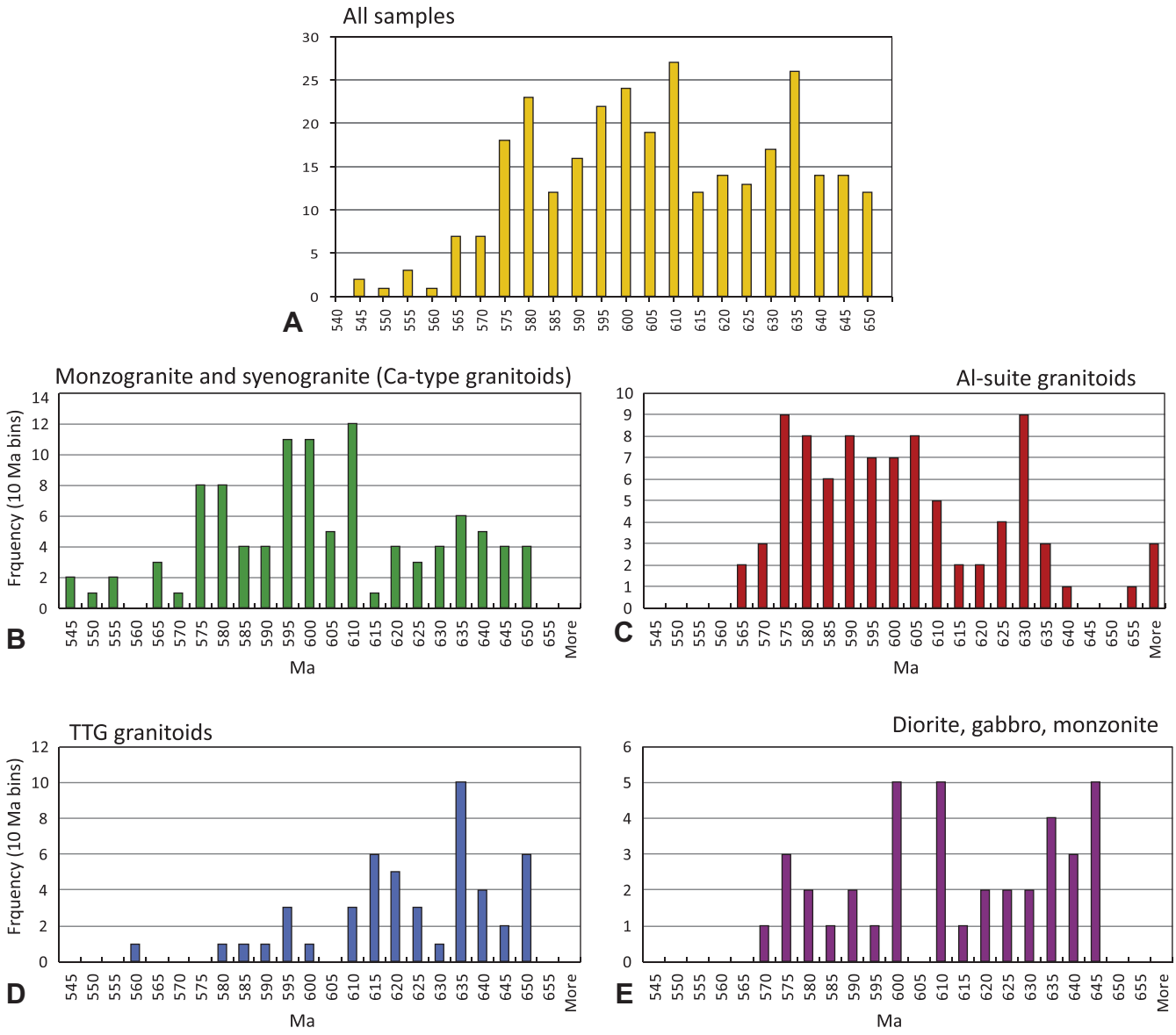

Fig. 7. Frequency plot of crystallization ages for selected groups of late Cryogenian–Ediacaran plutonic rocks in the ANS. Histograms plotted from U–Pb conventional, U–Pb ion-probe, and Rb–Sr whole rock crystallization ages listed in Appendix A. (A) All the data. (B) Chiefly monzogranite and syenogranite samples although some sampled plutons are composite and include granodiorite. (C) Chiefly alkali-feldspar and alkali-granite, but includes some syenogranite samples. (D) Chiefly trondhjemite, tonalite, and granodiorite samples, but includes some monzogranite. (E) Diorite, gabbro, and monzonite samples. The data are biased in favor of granite samples as being the most productive rocks for zircons and a deliberate focus of research interest, but the histograms are consistent with geologic observation that granite dominates late Cryogenian–Ediacaran magmatism in the ANS. The data also suggest an increase in the abundance of Al-type granitoids after about 610 Ma and a decrease in the abundance of Ca-type granitoids. The abundance of TTG samples reflects arc-type magmatism in the Ar Rayn terrane. Note the presence of diorite, gabbro, and monzonite throughout the period.

1986), crops out in a series of basins, 20–50 km wide, that are offset by as much as 50 km from each other by Najd faults. Prior to faulting, they probably formed a north-trending continuous basin more than 600 km long. The Bani Ghayy group is dated at ~620 Ma (Stacey and Agar, 1985, conventional U–Pb zircon age in rhyolite; Fleck et al., 1980, Rb–Sr whole-rock andesite age), although the group is intruded by quartz porphyry dated at 646 ± 11 Ma (Doebrich et al., 2004), which suggests that the maximum deposition age may be older than indicated by the direct dating; the group is listed in Table 2 as ~650–620 Ma. In places, the Bani Ghayy and Murdama groups are in virtual juxtaposition, and not all workers accept that they represent separate distinct lithostratigraphic units, referring to both as "Murdama group" (Brown et al., 1989). At issue is the extent to which the different lithologic compositions and depositional environments of the Murdama and Bani Ghayy groups warrant using separate lithostratigraphic names, a question that requires future assessment by stratigraphers.

The Bani Ghayy group contains polymict conglomerate, tuffaceous wacke, siltstone, limestone as much as 1000 m thick, and a bimodal sequence of porphyritic rhyolite, basalt, and andesite flows and tuffs as much as 1000 m thick (Pellaton, 1985; Agar, 1986; Kattan and Harire, 2000). Agar (1986) interprets the Bani Ghayy basin to be a fault-bounded graben. One of the bounding faults is exposed as a steeply, east-dipping serpentinite-decorated reverse fault (the Bi'r Tawilah fault shown on Fig. 15B) that is currently being explored for orogenic gold. Folds in the Bani Ghayy group indicate E–W shortening similar to that implied by folding in the Murdama basins.

The *Fatima group* crops out in a northeast-trending basin in the Jiddah terrane (Fig. 7). It contains conglomerate, sandstone, rhyolite, and basalt, and a considerable amount of limestone

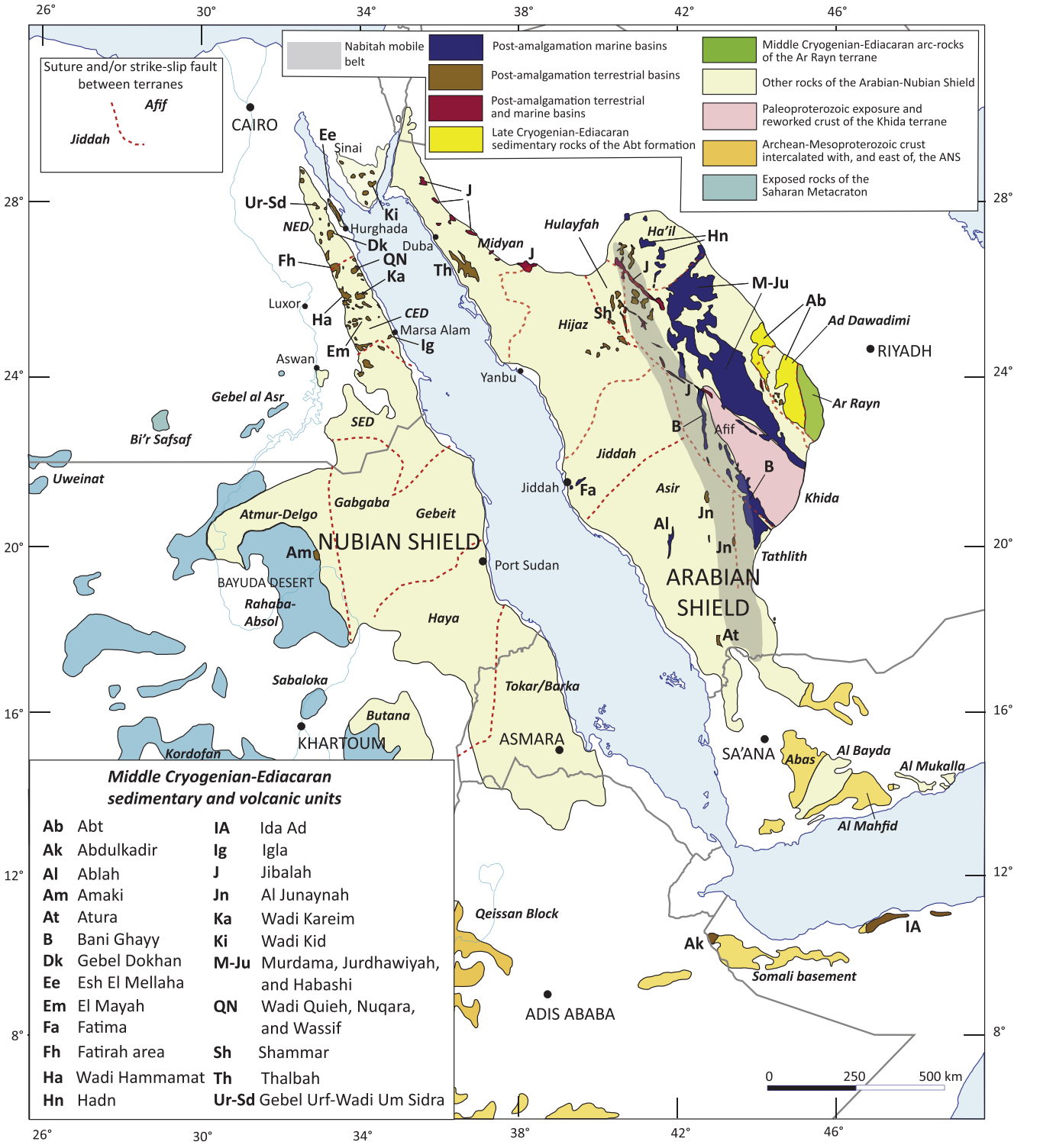

Fig. 8. Middle Cryogenian–Ediacaran sedimentary and volcanic assemblages in the Arabian–Nubian Shield. These assemblages mostly crop out in post-amalgamation basins, unconformable on newly amalgamated arc terranes. Exceptions are the Abt formation (Ab) and the arc rocks of the Ar Rayn terrane, which are treated as late Cryogenian–Ediacaran terranes rather than post-amalgamation basins. The figure includes some post-amalgamation assemblages that are middle Cryogenian (680–650 Ma) and older than the time period of this review, but are shown here for completeness.

with abundant crypalgalaminates, stromatolites, and archeocyathid biomicrites that may have been deposited in a stable shallow littoral-marine platform (Basahel et al., 1984). On the basis of Rb–Sr whole-rock ages from basalt, andesite, and rhyolite, the group is inferred to be about 685 Ma (Darbyshire et al., 1983), but Basahel et al. (1984) argue that its organic remains imply a Lower Cambrian age. From what is now known about the youngest rocks of the shield elsewhere, this seems unlikely. It is possible that the Fatima group correlates with the Jibalah (580–560 Ma), but this needs to be substantiated. The Fatima group is folded and was down faulted along the Fatima shear zone.

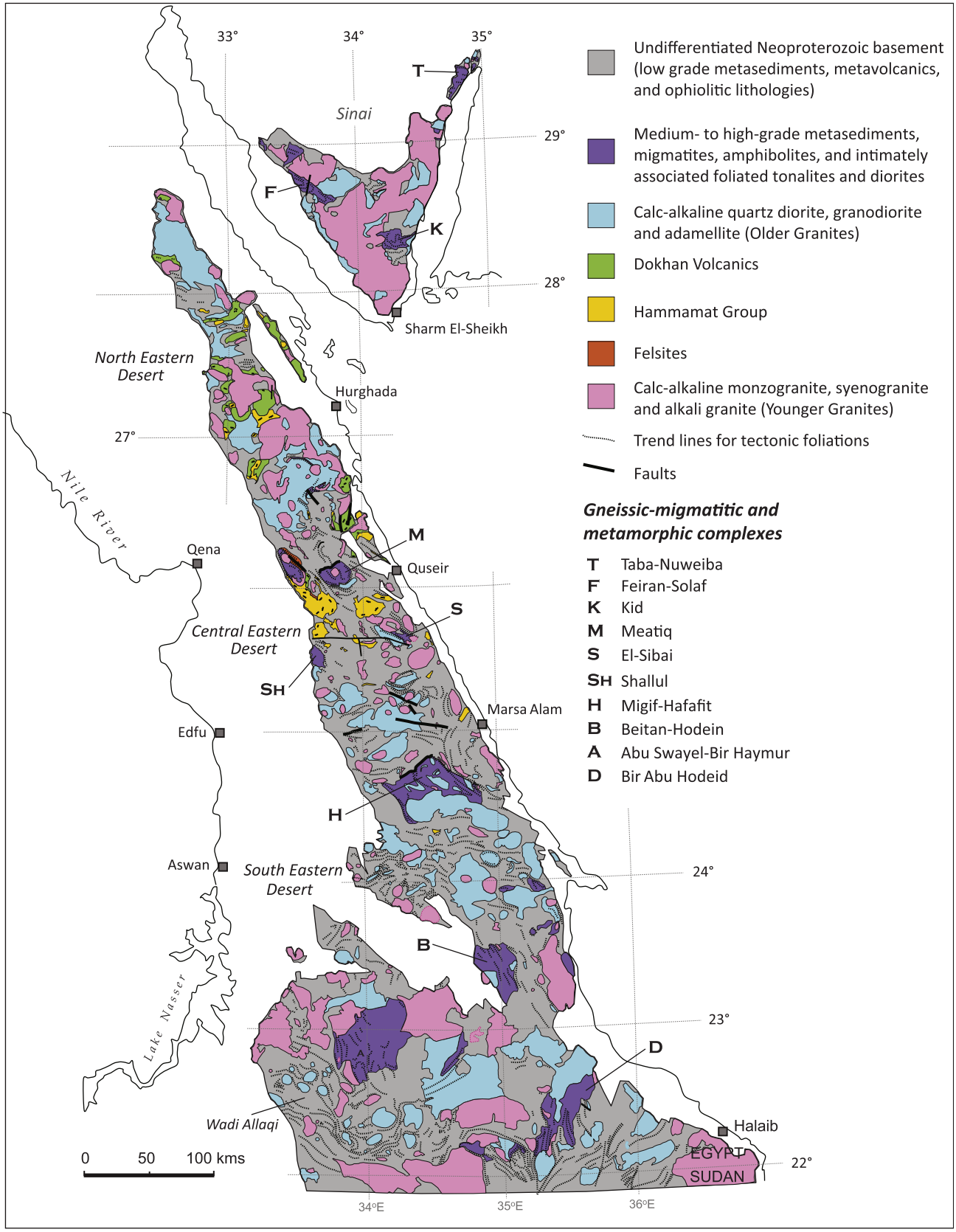

Fig. 9. Geologic map of the Eastern Desert and Sinai showing the distribution of the main geologic units and broad structural trends. Notice also the location of gneisses. Compiled and edited by A. Fowler from EGPC/CONOC Coral (1987) and Geological Survey of Egypt (EGSMA) 1:250,000 Geological Map series, 1992 to 2001.

Table 2
Middle Cryogenian–Ediacaran (650–542 Ma) sedimentary and volcanic successions in the Arabian–Nubian Shield. Apart from the Abt formation, these rocks occupy post-amalgamation basins. The basins are generally named after the deposit that fills them except for basins in the Eastern Desert, Egypt, which are individually named (see Fig. 7).

Name	Age/age range(Ma)	Comment	Depositional environment	Reference
Thalbah group	660–620	Not directly dated; unconformable on Zaam group and Imdan complex (660 ± 4 Ma) and intruded by Liban complex (621 ± 7 Ma)	Terrestrial: post-amalgamation basin	Davies (1985)
Afif formation and Murdama group	650–625	Minimum age reasonably well constrained; maximum age uncertain. Comprise largest post-amalgamation basin in ANS	Marine: post-amalgamation basin	Cole (1988), Cole and Hedge (1986), Greene (1993), Wallace (1986) and Kennedy et al. (2010)
Atura formation	<650 to >640	Not directly dated; small, strongly deformed and metamorphosed basin in the Asir terrane	Terrestrial: post-amalgamation basin	Fairer (1985)
Bani Ghayy group	~650–620	Depositional age weakly constrained	Marine: post-amalgamation basin	Agar (1986), Doebrich et al. (2004)
Ablah group	640–615	Directly dated at 641 ± 4 Ma and 613 ± 7 Ma	Marine: post-amalgamation basin	Genna et al. (1999) and Johnson et al. (2001)
Al Junaynah group	<640	Unconformable on Asir terrane supracrustals and ~640 Ma granites along Nabitah fault zone; small north-trending basins along the Nabitah and adjacent shear zones	Terrestrial: post-amalgamation basin	Not directly dated
Hibshi formation	632 ± 5	Unconformable on the Hail terrane; in fault contact with Murdama group; directly dated at 632 ± 5 Ma	Terrestrial: post-amalgamation basin	Cole and Hedge (1986) and Williams et al. (1986)
Shammar group	630–625	Unconformable on Nuqrah assemblage (~820 Ma) and intruded by granites (~630 Ma)	Terrestrial: post-amalgamation basin	Calvez and Kemp (1987) and Kemp (1996, 1998)
Amaki Series	Uncertain	Pull apart associated with transpression–transtension on the Keraf suture	Terrestrial: post-amalgamation basin	Ries et al. (1985) and Abdelsalam and Stern (1996)
Abt formation	$\gtrsim$ 620	Stratigraphic base and top unknown; intruded by granite plutons 605–565 Ma: sedimentary sequence comprising the Ad Dawadimi terrane	Marine: tectonic setting debated, possibly forearc basin with respect to the Al Amar arc	Delfour (1982), Kennedy et al. (2005, 2011), Lewis (2009) and Cox et al. (2011)
Hadn formation	~614–600	Unconformable on crystalline rocks of the Ha'il terrane and intruded by plutons of the Idah suite (620–615 Ma): epiclastic and calc-alkaline volcanic rocks	Terrestrial: post-amalgamation basin	Cole and Hedge (1986), Johnson (2006) and Kennedy et al. (2010)
Jurdhawiyah group	612–594	Unconformable on Murdama group; directly dated in the An Nir basin. Terrigenous clastic and volcanic deposit	Terrestrial: post-amalgamation basin	Cole (1988), Cole and Hedge (1986) and Kennedy et al. (2004, 2005)
Dokhan Volcanics and Hammamat Group	616–585	Unconformable on Older Metavolcanics and Older Granite; intruded by or synchronous with Younger Granites	Terrestrial: post-amalgamation basin	Willis et al. (1988), Wilde and Youssef (2000) and Breitkreuz et al. (2010)
Jibalah group	~590–560	Age well constrained by direct dating of zircon clasts and igneous (tuffaceous) grains. Southeast of Al 'Ula, is unconformably overlain by the newly recognized Kurayshah group, the youngest Ediacaran succession on the Arabian Shield	Terrestrial–marine: post-amalgamation basin	Delfour (1970), Matsah and Kusky (1999), Nicholson et al. (2008), Vickers-Rich et al. (2010), Miller et al. (2008) and Nettle (2009)
Saramuj Conglomerate, Haiyala Volcaniclastic Formation, Wadi Araba volcanic suite, and Wadi Abu Barqa Formation	~555–550	Age constrained by Rb–Sr whole rock isochron for alkali-feldspar rhyolite in the Wadi Araba volcanic suite (553 ± 11 Ma) and trachybasalt (545 ± 13 Ma) and andesite (550 ± 13) dikes that intrude the layered rocks	Terrestrial; locally shallow marine	Jarrar et al. (1992)

3.2. Terrestrial basins

Post-amalgamation basins in the northwestern part of the ANS are terrestrial suggesting a location more elevated and(or) farther from the sea than the marine basins in the east. One of the oldest and largest is the *Thalbah basin* (100 km by 45 km), occupied by the Thalbah group (Davies, 1985), in the Midyan terrane in the northwestern part of the Arabian Shield. The Thalbah is entirely epiclastic; other terrestrial basins contain volcanic and epiclastic sequences, such as the Dokhan Volcanics and the Hammamat Group of Egypt.

The Thalbah group (>5000 m) comprises polymict conglomerate, sandstone, and siltstone. Neither limestone nor volcanic rocks are present. The group is unconformable on the arc-related Zaam group and Imdan plutonic complex (660 ± 4 Ma) and intruded by the Liban complex (621 ± 7 Ma), which brackets deposition between 660 Ma and 620 Ma. The rocks are moderately folded, with bedding dips between <10° and 70°. Cleavage is well developed, but the rocks are barely metamorphosed except along the Qazaz shear zone where conglomerate clasts are stretched and the rock is changed to paragneiss, with foliation and mineral/stretching lineations conformable with those in orthogneiss in the shear zone. The Thalbah group reflects rapid deposition of rudaceous and arenaceous sediment interrupted by quieter intervals of fine grained sedimentation close to an emerging and strongly eroded mountainous hinterland (Genna et al., 2002). Massive conglomerates suggest mass flow deposition; bedded conglomerates and sandstones indicate fluvial deposition.

The *Dokhan Volcanics* and *Hammamat Group* crop out in small terrestrial post-amalgamation basins in the Eastern Desert; limestone is absent. They have been recognized in the Eastern Desert for many years (Akkad and El Ramly, 1958; El Ramly, 1972) and are described by an extensive literature. The Dokhan Volcanics succession varies in thickness from basin to basin, ranging from a few tens of meters to 1300 m (Eliwa et al., 2006). The Hammamat Group ranges from about 4000 m thick along Wadi Hammamat

in the type Hammamat basin (Abd El-Wahed, 2009) to about 7500 m in the Kareim basin (Fritz and Messner, 1999).

The proportions of volcanic and sedimentary rocks vary from basin to basin. Some contain only volcanic rocks, for example, the type Dokhan Volcanics basin; others are entirely sedimentary, such as the type Hammamat Group basin; yet other basins contain both volcanic and sedimentary rocks. Because of the varied distributions of these volcanic and sedimentary rocks and different relationships in basins where both rock types occur, the stratigraphy of the Dokhan Volcanics and Hammamat Group is debated. Some workers consider that the Hammamat Group underlies the Dokhan Volcanics (e.g., Stern and Hedge, 1985; Willis et al., 1988); others believe that the Hammamat overlies the Dokhan (e.g., Dardir and Abu Zeid, 1972; El Ramly, 1972; Akkad and Noweir, 1980; Ries et al., 1983; Hassan and Hashad, 1990); yet others infer that the two interfinger and are essentially contemporaneous (Ressetar and Monrad, 1983; Stern et al., 1984; El-Gaby et al., 1989; Eliwa et al., 2010). A problem is that the Hammamat Group and Dokhan Volcanics are defined on the basis of facies, whereas deposition took place in a dynamic setting around isolated volcanic centers and basin systems with different structural controls and different ages (Breitkreuz et al., 2010), so that the two facies should not be expected to occur in the same relative stratigraphic position in every basin.

Both units are Ediacaran. Recent SHRIMP U–Pb dating of zircons from ignimbrite and subvolcanic rhyolite (Breitkreuz et al., 2010) and previous Rb–Sr whole-rock ages (Stern, 1979; Abdel-Rahman and Doig, 1987), U–Pb conventional zircon ages (Stern and Hedge, 1985), and SHRIMP zircon ages (Wilde and Youssef, 2000) establish that the Dokhan Volcanics erupted between ~630 and ~592 Ma. An older weighted U–Pb SHRIMP age of uncertain significance is reported by Wilde and Youssef (2000) (685 ± 16 Ma) from a zircon core. Detrital zircons from the base of the Hammamat succession in the Gebel Um Tawat area, northern Eastern Desert, Egypt, yield a U–Pb SHRIMP age of about 585 Ma, and Wilde and Youssef (2000) infer that the group overall was deposited between about 593 and 579 Ma.

Wilde and Youssef (2002) suggest that the Hammamat Group was deposited in a major fluvial system of continental proportions that linked the various basins, and possibly linked to similar successions in Sinai and Jordan; other workers infer that the group was deposited in isolated, fault-bounded basins (Grothaus et al., 1979; Abdeen and Greiling, 2005). These are variously classified as a foreland basin, in the case of the type Hammamat basin (Fritz et al., 1996), intermontane basins in the cases of the Kareim, Queih, and Igla basins, for example (Abd El-Wahed, 2009), a strike-slip pull-apart basin, in the case of the El Mayah basin (Shalaby et al., 2006), and fault-bounded basins (Abdeen and Greiling, 2005). The range of inferred structural controls included thrusting, normal faulting, strike-slip faulting, N–S to NW–SE extension, and magmatic doming. In the type Hammamat basin, the Hammamat Group was deformed and metamorphosed and thrust over younger Dokhan Volcanics, perhaps as a result of deposition in a piggy-back foreland basin in front of a SW-propagating thrust front (Andresen et al., 2009). Both Hammamat and Dokhan units were affected by rapid hinterland uplift at about 595–588 Ma (Fritz et al., 1996; Loizenbauer et al., 2001) and subsequently intruded by the 596 Ma Um Had granite (Andresen et al., 2009). Initial subsidence of the Hammamat Group in the Kareim basin was associated with the formation of strike-slip faults around the Sibai gneiss dome as this was beginning to be exhumed (~650 Ma) (Bregar, 1996; Bregar et al., 2002) and terminal fanglomerate deposition was associated with the intrusion of young granite at about 580 Ma (Hassan and Hashad, 1990; Fritz and Messner, 1999). The El Mayah basin (Shalaby et al., 2006) was initiated as a fault-bounded half-graben and later evolved into a pull-apart basin at a prominent bend in a sinistral shear system of the Najd fault (see the location of the basin shown in Fig. 16).

The Hammamat Group typically comprises greenish-gray siltstone, lithic sandstone, and polymict conglomerate containing pebble-sized clasts of quartz, foliated granite, purple Dokhan type andesite, felsic volcanic rock, basalt, quartz porphyry, and undeformed pink granites. The Gebel El Urf basin, which contains both Hammamat and Dokhan facies, comprises alluvial-fan deposits, fluvial braided flood-plain deposits, deep lacustrine deposits, lacustrine-delta deposits, andesitic phreatomagmatic volcanic deposits, explosive pyroclastic deposits, and coherent bodies of lava flows, sills, and dikes (Eliwa et al., 2010). It is inferred that the rocks accumulated in a structurally controlled intermontane basin, beginning with alluvial-fan conglomerates and sandstone eroded from flanking high mountains, followed by the development of a deep lake, perhaps as a result of down faulting. Shrinkage of the lake is marked by a return of high-energy arenaceous and rudaceous sedimentation concurrent with the onset of silica-rich and silica-poor volcanic centers leading to the formation of volcanogenic mass flow deposits, hyaloclastic deposits, and lavas. The terminal history of the basin was marked by at least two large ignimbrite-forming caldera eruptions. The original margins of the basin are unknown. The succession has been folded into a broad E-trending syncline, the southern limb of which is metamorphosed in its basal part.

The Dokhan Volcanics typically include basaltic andesite, andesite, dacite, and rhyolite that some consider to be a bimodal suite (Stern and Gottfried, 1986; Mohamed et al., 2000) although this conclusion has been challenged (Eliwa et al., 2006). The rocks are enriched in LILEs (Rb, Ba, K, Th, Ce) relative to high field strength elements (Nb, Zr, P, Ti) and show strong affinity to calc-alkaline subduction-related rocks. However, their undeformed character, their temporal and spatial association with posttectonic A-type granite, and their high Zr/Y suggest that their emplacement followed the cessation of subduction in the Eastern Desert in an extensional, within-plate setting. Equivalent felsic volcanic rocks in the Wadi Kid area, Sinai, have strong high-K calc-alkaline affinity, with relative enrichment in total alkalis, Ba, Y, Zr and total REEs, depletion in Sr, and a LREE-enriched REE patterns with significant negative Eu anomalies. On the basis of these geochemical characteristics, which are compatible with both orogenic arc-type and anorogenic within-plate environments, El-Bialy (2010) suggests that they were erupted in a transitional "post-collisional tectonic setting". Mohamed et al. (2000) argue that their major and trace-element variations are consistent with their formation by partial melting of an enriched subcontinental lithospheric mantle followed by a limited amount of low-pressure fractional crystallization of olivine and pyroxene prior to eruption. In contrast, Eliwa et al. (2006) concluded that the trace element compositions of Dokhan alkali basalt, calc-alkaline, and adakitic lavas indicated that Dokhan magmas reflected melting of hot oceanic crust due to subduction of a hot oceanic ridge.

3.3. Mixed terrestrial–marine basins

This type of post-amalgamation basin in the ANS is typified by the *Jibalah group* (Delfour, 1970) (alternative spellings: J'balah, Jubaylah). The group crops out in small, isolated synclinorial basins adjacent to northwest-trending Najd faults in the northern part of the Arabian Shield (Fig. 10). The Jibalah rocks are folded and bedding dips may be steep but the group is barely metamorphosed. Disharmonic, en-echelon, and S- and Z-shaped asymmetric folds in some basins probably formed under conditions of sinistral and dextral simple shear (Kusky and Matsah, 2003). Matsah and Kusky (2001) and Kusky and Matsah (2003) suggested that some of these basins, such as the Jifn Basin along the Halaban-Zarghat fault,

formed as pull-apart basins during early dextral stages of motion along the Najd faults, and were then cut by structures related to a later sinistral motion along the faults.

The Jibalah group, the recently recognized Kurayshah Group (Nicholson et al., 2008), which overlies the Jibalah group in the Al 'Ula area of Saudi Arabia, and the broadly coeval Saramuj Conglomerate, Haiyala Volcaniclastics, Wadi Araba volcanic rocks (Jarrar et al., 1992), and the Wadi Abu Barqa Formation (Bandel and Shinaq, 2003) in Jordan are the youngest depositional units in the ANS. They unconformably overlie all other rocks in the Shield, with the exception of some posttectonic dikes, and are unconformably overlain by Lower Cambrian sandstone. Zircons from tuff beds in the Jibalah group yield ages of 560 ± 4 Ma (Vickers-Rich et al., 2010), 599 ± 5 Ma (core) and 570 ± 5 Ma (rim) (Kennedy et al., 2011), 588–600 Ma (Nicholson et al., 2008), and 568–585 Ma (Nettle, 2009) suggesting deposition between ~590 and 560 Ma. The minimum deposition age for Jibalah rocks in the north-central part of the Arabian Shield is constrained by a felsite dike dated at 577 ± 6 Ma that intrudes the group (Kusky and Matsah, 2003).

The group is characterized by maroon and purple sandstone, siltstone, and polymict conglomerate, cherty and siliceous stromatolitic limestone and calcareous argillite, dacite and rhyolite. In some basins, thick fanglomerates along the faulted sides of the basins suggest deposition during active faulting (Kusky and Matsah, 2003). Volcanic rocks and limestone are absent from some Jibalah-group basins, but the clastic deposits are always present. The purple-brown coloration of many of the Jibalah rocks, the algal-mat and stromatolitic biohermal carbonates, and sedimentary structures including ripple marks, graded bedding, and cross lamination indicate deposition in shallow water.

At Jabal Jibalah in the north-central part of the Arabian Shield (Fig. 10), the group is more than 3300 m thick; in the Antaq basin, a half graben or pull-apart basin 45 km by 10 km in extent, the group is as much as 2000 m thick (Nettle, 2009). Small Jibalah group basins in the northwestern Arabian Shield are similar (Hadley, 1974; Nicholson et al., 2008; Miller et al., 2008; Grainger and Hanif, 1989; Vickers-Rich et al., 2010). Recent work has identified matrix-supported boulders, cobbles, and possible dropstones in conglomeratic sandstone in some of the basins that may represent glaciogenic diamictite although most conglomeratic units are fanglomerate (Kusky and Matsah, 2003; Miller et al., 2008; Vickers-Rich et al., 2010).

The appearance of carbonates in the Jibalah basins marks a gradual change from a restricted non-marine environment to an increasingly marine environment. Microbial-mat structures in the carbonates are widespread, and the group has been recently searched for Ediacaran macrofossils (Miller et al., 2008; Vickers-Rich et al., 2010; Nettle, 2009). Exposures in basins in the northwestern Arabian Shield contain *Beltanelloides*-like structures that may represent algae or metazoans; a possible *Pteridinium* imprint and possible trails or burrows (Miller et al., 2008); and helically coiled tubular filaments of *Obruchevella parva* and the conical stromatolite *Conophyton* (Cloud et al., 1979). More recently, a fragment of *Charniodiscus* sp. and three possible specimens of *Aspidella* sp. have been reported from the Jibalah group in the Antaq basin in the far eastern Arabian Shield (Nettle, 2009). Cyanobacterial mats extensively developed during deposition of the Wadi Abu Barqa Formation in Jordan, which is broadly correlative with the Jibalah group (Bandel and Shinaq, 2003). $^{87}Sr/^{86}Sr$ values measured in some limestones are between 0.704 and 0.706, well below the range of reported Ediacaran marine values and suggesting significant Sr contribution from igneous rocks recently extracted from the mantle (Miller et al., 2008). Carbon isotopes in the carbonates, on the other hand, with $\delta^{13}C_{carb}$ near 2‰, are consistent with a marine environment (Miller et al., 2008). Nicholson et al. (2008) interpret Jibalah limestone in the Al 'Ula area as a distal marine deposit. Cloud et al. (1979) comment that the brecciated and micro-channeled appearance of fossiliferous rock in the Rubtayn basin, in the northwestern Arabian Shield, its locally dolomitic nature, and the prevalence of cryptalgalaminate favor a very shallow, locally turbulent, and perhaps episodically exposed marine or marginal marine setting. Diamictite and dropstone as well as the geochronology of the group are consistent with deposition during or sometime after the Gaskiers (~580 Ma) Ediacaran glacial event.

Two contrasting depositional models are proposed for the Jibalah group. One envisages that the group was continuously deposited over a large part of the northern Shield as the result of a shallow marine incursion, and is now preserved in younger grabens, having been eroded in other places. Based on recent mapping and sampling, Nicholson et al. (2008) recognize the same stratigraphy in several of the Jibalah basins on the Arabian Shield consistent with the interpretation that the unit was originally widespread. The facies recognized by Nicholson et al. (2008) indicates deposition within a single, laterally continuous basin that evolved from proximal fluvial conditions at its base to a marine shelf setting at the top. The other model envisages that the Jibalah group was never regionally extensive but was deposited syntectonically in fault-controlled basins under fluvial to shallow-marine or lacustrine conditions (e.g., Delfour, 1977; Husseini, 1988; Al-Husseini, 2000; Kusky and Matsah, 2003; Nettle, 2009). In terms of a fault-controlled basin model, the Al Jifn basin (north-central Arabian Shield) is inferred to have developed at a releasing bend along the Halaban-Zarghat fault during a period of dextral shear (Matsah and Kusky, 2001; Kusky and Matsah, 2003). The Al Kibdi (eastern Arabian Shield) basin is located between two left-stepping strike-slip splays of the Ar Rika fault and is a pull-apart basin that formed during sinistral shear. The Antaq basin (eastern Arabian Shield) is a half-graben that appears to have formed as a result of normal dip-slip movement on the hanging wall, perhaps during E–W-directed extension. The Rubtayn basin (NW Arabian Shield) consists of fault blocks and grabens depressed as a result of subsidence along boundary faults (Hadley, 1974).

4. Late Cryogenian–Ediacaran magmatism

Igneous activity was very important in the Late Cryogenian-Ediacaran evolution of the ANS, and included both intrusive and extrusive events. Neoproterozoic plutonic rocks form 42% of the exposed surface in the Arabian Shield (Fig. 11) (15% monzogranite and syenogranite, 4% alkali-feldspar granite, and 8%, 7%, 6%, and 2%, respectively, granodiorite, tonalitic rocks, dioritic rocks, and gabbro) (Stoeser, 1986). The basement of the Egyptian Eastern Desert consists of between 40% and 80% plutonic rock, mainly granite (Hussein et al., 1982; Stern and Hedge, 1985) (Fig. 9). A particular feature of the ANS is an abundance of A-type granitoids (A for anorogenic), especially alkali granite; in fact it is said that the region contains one of the largest fields of alkali granite in the world (Stoeser, 1986). A-type granites have mildly alkaline geochemistry, and are interpreted to have crystallized under low water fugacities. They have high Fe/Mg, (K + Na)/Al, and K/Na, abundant F, Zr, Nb, Ga, REE, Y, and Zn, and low Mg, Ca, Al, Cr, and Ni (Collins et al., 1982; Creaser et al., 1991). Among these rocks, alkali granite is characterized by containing alkali (sodic and sodic–calcic) amphibole and/or pyroxene (Streckeisen, 1976), the presence of such minerals being evidence that the parental melt was peralkaline in composition. On the IUGS QAP diagram (Streckeisen, 1976), alkali-feldspar granite contains about 90% or more (on a normalized feldspar scale) alkali feldspar, including plagioclase with anorthite content less than An_{05}. In practice, difficulties and ambiguities were found when applying the name "alkali granite" to granitoids in the Arabian Shield, but guidelines used for many of the granite

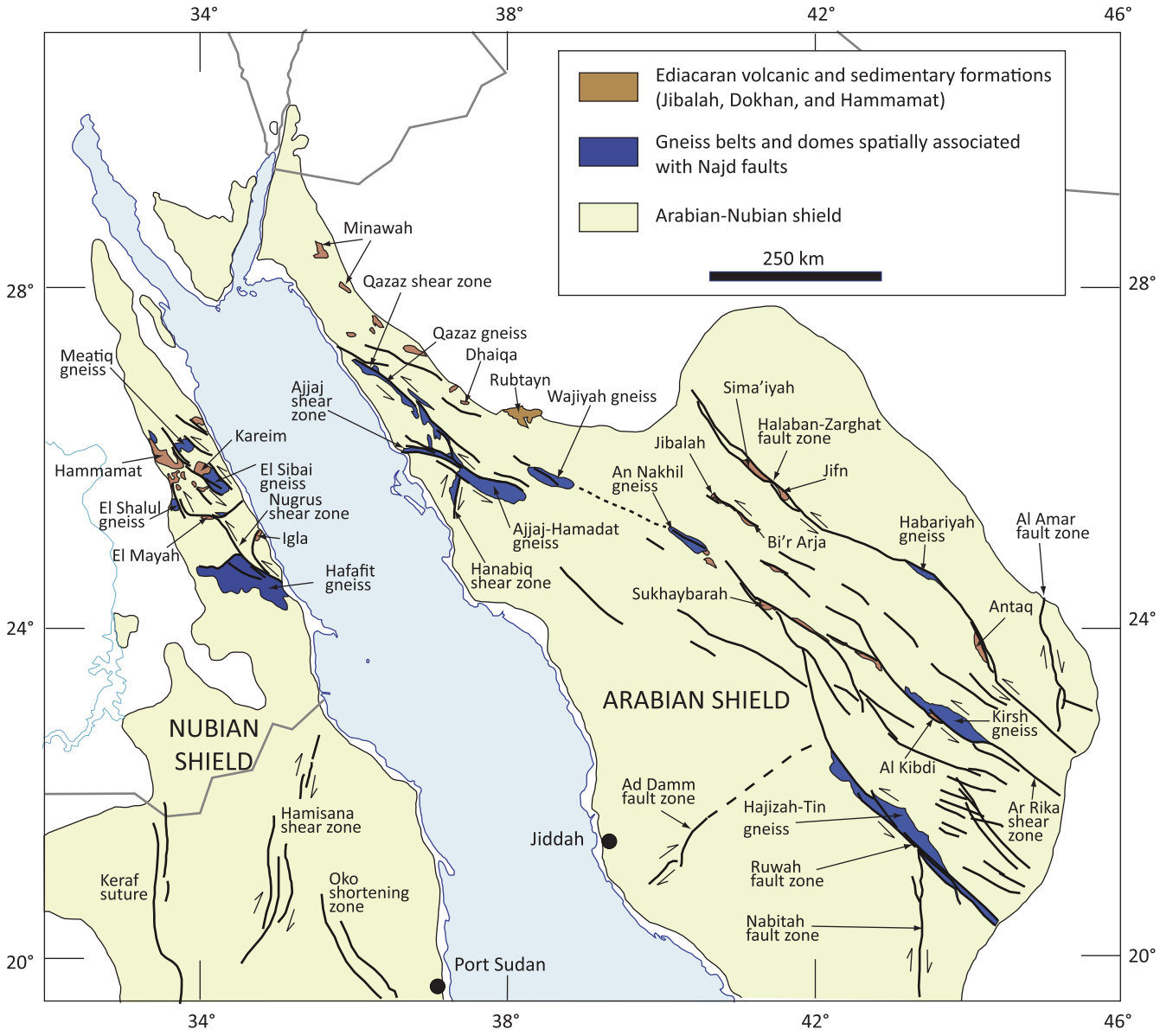

Fig. 10. Simplified map showing the spatial and genetic(?) relationships in the northern part of the Arabian–Nubian Shield between: (1) northwest-trending faults of the Najd fault system; (2) broadly contemporary shear zones of other orientations; (3) Ediacaran volcanic and sedimentary deposits of the Jibalah, Dokhan, and Hammamat groups; and (4) antiforms, domes, and linear belts of strongly deformed metasedimentary, metavolcanic, and metaplutonic rocks (paragneiss and orthogneiss). Names refer to fault zones, shear zones, depositional basins, and bodies of gneiss (compiled from Johnson and Woldehaimanot (2003), Abdelsalam and Stern (1996) and Shalaby et al. (2006)). Arrows show sense of shear.

studies conducted in the shield in the 1980s are set out by Ramsay et al. (1986).

The ANS late Cryogenian–Ediacaran intrusion styles range from sills, dikes, and stocks to plutons and batholiths, and the intrusions range from those with homogeneous compositions, to nested complexes, and to ring complexes. They were emplaced at mid- to high-levels in the crust, and some granitic intrusions can be seen in the field to have breached the surface and to be flanked by coeval lavas, such as in the east-central part of the Arabian Shield where the Wasit formation forms a volcanic pile of felsic tuffs and rhyolite overlying a posttectonic syenite (Pellaton, 1985). The late Cryogenian–Ediacaran plutons are typically discordant with respect to already deformed and metamorphosed country rocks, mostly lack penetrative deformation fabrics, and have the general character of late- to posttectonic intrusions. Exceptions are bodies of late Cryogenian–Ediacaran orthogneiss along Najd faults in the Arabian Shield, and in and around gneiss domes in the Eastern Desert that were syntectonically intruded during shearing and thrusting. Many plutons, particularly alkali-feldspar granites, weather out as prominent positive topographic features, elevated as inselbergs and enormous massifs above the surrounding rocks (Fig. 12); other plutons, particularly granodiorite and monzogranite, weather more readily and crop out as low-relief surfaces covered in grus.

4.1. Granitoids

Geographically, late Cryogenian–Ediacaran plutonic rocks are most abundant in the north and northeast of the ANS (Fig. 13). The reason(s) for this distribution is uncertain. It may reflect greater recent erosion of the ANS in the south than in the north because of post-Oligocene uplift over the Afar hotspot or a

greater degree of end-Precambrian uplift and peneplanation in the south than the north, resulting in the removal of epizonal plutons in the southern ANS. Other comparable N–S contrasts are evident in the distribution of post-amalgamation basins (Fig. 8) and late Cryogenian–Ediacaran gneisses, and in the orientations and origins of shear zones and shortening zones (see Fig. 19).

On the basis of the geochronologic data shown in Fig. 7, it is evident that from the perspective of the ANS as a whole, late Cryogenian–Ediacaran magmatism was quasi-continuous, although punctuated by surges in activity as well as systematic increase in LILE abundances with time. A commonly accepted view of Cryogenian–Ediacaran ANS magmatism is that it evolved from arc-related tholeiite and calc-alkaline TTG assemblages, to collisional-related calc-alkaline TTG and granite assemblages, to post-collisional within-plate A-type granitoids that formed in extensional regimes during orogenic collapse (Stern and Hedge, 1985; Beyth et al., 1994; Moghazi et al., 1998; Garfunkel, 1999; Jarrar et al., 2003; Mushkin et al., 2003; Moussa et al., 2008). The transition from collision to extension, manifested by the emplacement of granites in association with dike swarms and volcanic rocks extruded in molasse-type basins, is commonly dated about 610 Ma (Beyth et al., 1994).

Such a transitional model of magmatism has a long history, reflected in the Egyptian stratigraphic divisions of "Older granites" and "Younger granites" (Hume, 1934; El Ramly and Akaad, 1960; Akkad and Noweir, 1980; Bentor, 1985) and is, to some extent, supported by precise U–Pb zircon dating. In the Eastern Desert, for example, Youssef (2005) obtained SHRIMP U–Pb ages of ~755–655 Ma for "Older granites" at Gebel Gattar and 576 ± 6 Ma and 594 ± 3 Ma for the "Younger granites". Moussa et al. (2008) obtained SHRIMP U–Pb zircon ages of 652 ± 3 Ma for a granodiorite and ~595–605 Ma for later granitoids. Parts of the eastern Arabian Shield also provide evidence of a temporal change in granitoid type, with calc-alkaline assemblage of granodiorite, tonalite, trondhjemite, diorite, minor gabbro and local monzogranite, syenogranite and alkali-feldspar granite (Kishaybi and Idah suites) emplaced in the Afif terrane between 645–615 Ma and strongly fractionated peralkaline, peraluminous, and related leucocratic granites (Abanat suite) emplaced at 585–570 Ma (Cole and Hedge, 1986).

However, recent work challenges the traditional view of a straightforward temporal transition. Lundmark et al. (2011), using newly obtained U–Pb ID-TIMS ages and earlier U–Pb conventional, ID-TIMS and SHRIMP ages in the Central Eastern Desert (CED), Egypt, identify six pulses at: (1) 705–680 Ma; (2) ~660 Ma; (3) 635–630 Ma; (4) 610–604 Ma; (5) 599–590 Ma: and (6) 550–540 Ma. The first three pulses are synorogenic; pulses 4 and 5 record exhumation of mid-crustal gneisses, and pulse 6 postdates orogeny. In NE Sudan, Stern and Abdelsalam (1998) noted that plutons defined an early peak in LILE abundances at ~740 Ma followed by voluminous intrusion of ~690–720 Ma low-K TTG suites, and then by plutons that became increasingly LILE-rich with time. In Arabia, alkali granites as old as 686 ± 26 Ma, 678 ± 10 Ma, and 640 ± 3 Ma are reported from the Hijaz and Asir terranes in the Arabian Shield (Duyverman et al., 1982; Cooper et al., 1979; Johnson et al., 2001), whereas elsewhere calc-alkaline and alkaline suites are both coeval and younger. The Sabaloka area, SW of the ANS, contains post-collisional high-K 605 ± 4 Ma calc-alkaline granite as well as 591 ± 5 Ma shoshonitic granite. Late-tectonic magmatism in the Tokar/Barka terrane in Eritrea includes contemporary medium- to high-K, I-type calc-alkaline granodiorite and granite (622 ± 1 Ma) and alkaline to shoshonitic syenite dikes (628 ± 4 Ma) and small plutons (Teklay et al., 2001) and broadly coeval posttectonic granodiorite (606 ± 1 Ma) and granite (613 ± 1 Ma, 612 ± 6 Ma) are found in Ethiopia (Miller et al., 2003; Avigad et al., 2007). These results identify magmatic episodes in the southern ANS that encompass coeval intrusive rocks of different chemistry and modal compositions, and are EAO examples of the shift from high-K calc-alkaline to shoshonitic or alkaline–peralkaline magmatism recognized in the final stages of orogeny in the Neoproterozoic belts of West Africa (Liégois et al., 1998).

In the northern ANS, coeval as well as transitional late Cryogenian–Ediacaran magmatism is recognized in the northern Midyan terrane (Jordan) and Sinai (Egypt and Israel). In southern Israel, Beyth et al. (1994) dated an I- to A-type transition at ~610 Ma. In Jordan, Jarrar et al. (2003) noted a transition at about 600 Ma between calc-alkaline gabbro to high-silica granite belonging to the 640–600 Ma Aqaba complex and alkali-calcic to alkali rocks belonging to the 600–560 Ma Araba complex, yet the Aqaba complex itself includes both mafic and felsic assemblages. The mafic assemblage consists of quartz-diorite, quartz-monzodiorite, monzodiorite, and monzogabbro (the Araba Mafic to Intermediate Suite: 595–570 Ma); the felsic assemblage of microgranite, alkali-feldspar granite and syenogranite (the Humrat–Feiran Suite: 568 Ma), another evidence of coeval mafic and felsic magmatism during the closing stage of ANS evolution.

Coeval calc-alkaline and alkaline Ediacaran granitoids likewise dominate basement outcrops in Sinai (El-Shafei and Kusky, 2003; Be'eri-Shlevin et al., 2009b; Ali et al., 2009). Be'eri-Shlevin et al. (2009b) sampled slightly deformed to mostly undeformed calc-alkaline granodiorite, monzogranite and minor gabbro and quartz-diorite, referred to as a CA2 suite (~635–590 Ma) and alkaline and peralkaline granites and monzodiorite forming an AL suite (~608–580 Ma). Rocks within the CA2 suite show a change from mafic to felsic magmatism, with a peak in granodiorite to granite magmatism at 610–600 Ma. AL-suite magmatism started contemporaneously with the peak in the CA2 granitic magmatism at about 608 Ma and continued until ~580 Ma (Be'eri-Shlevin et al., 2009b). Ali et al. (2009) sampled discordant, posttectonic calc-alkaline as well as alkaline suites of monzogranite, syenogranite, and alkali granite elsewhere in Sinai, and discovered that they all date between 594 and 579 Ma and show no temporal progression.

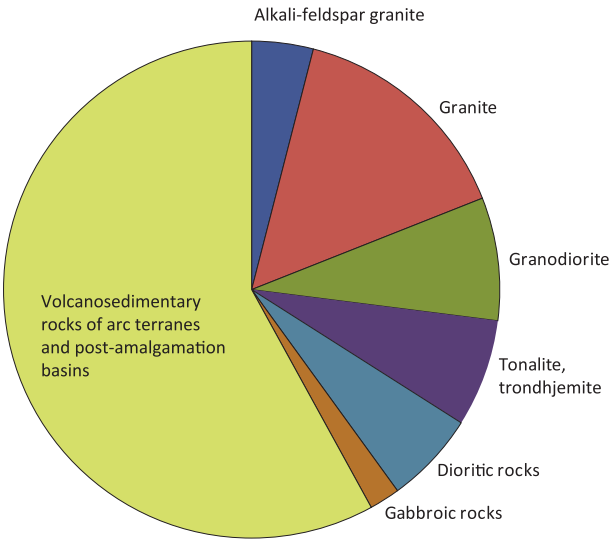

Fig. 11. Proportions of plutonic and other rocks in the Arabian Shield (after Stoeser, 1986). Orthogneiss does not figure as a separate category in this diagram because gneiss is calculated in terms of the protolith – thus dioritic gneiss is grouped with diorite; granite gneiss with granite, etc. Ultramafic rocks do not figure either, but amount to about 1%. The Nubian Shield has a similar composition except for a greater proportion of ultramafic rocks.

As these results indicate, the change from calc-alkaline to alkaline magmatism in the ANS was not instantaneous and cannot be neatly pinned at 610 Ma. Both types of magmatism occurred during the late orogenic extensional phase in the ANS and intrusions of both magma types are found juxtaposed in any given area. In places, the two magma types can be chronologically separated, with the calc-alkaline intrusions older than the alkaline, but in other places, the two overlap or are coeval. Similar associations between calc-alkaline and alkaline granitoids occur elsewhere in the world, because calc-alkaline magmatism is known to result from lithospheric extension in areas with a long history of previous subduction (Hooper et al., 1995), leading to the situation that both calc-alkaline and alkaline granitoids plot jointly in the post-collisional field on the Rb/Y + Nb discrimination diagram of Pearce (1996).

Late Cryogenian–Ediacaran magmatism in the Ar Rayn terrane in the eastern Arabian Shield reflects a different set of tectonic constraints (Doebrich et al., 2007). In this region, the plutonic rocks are divided into two partly coeval suites of (1) low-Al trondhjemite–tonalite–granodiorite (TTG suite) emplaced between 632 Ma and 616 Ma and (2) high-Al TTG/adakitic rocks emplaced between 689 and 617 Ma, and a suite of alkali-feldspar granite, two samples of which are dated at 607 ± 6 Ma and 583 ± 8 Ma (Doebrich et al., 2007). The TTG suites are arc-related and imply that subduction continued in the Ar Rayn terrane until at least about 615 Ma. The alkali-feldspar granite forms discordant plutons typical of a post-tectonic setting following the cessation of subduction.

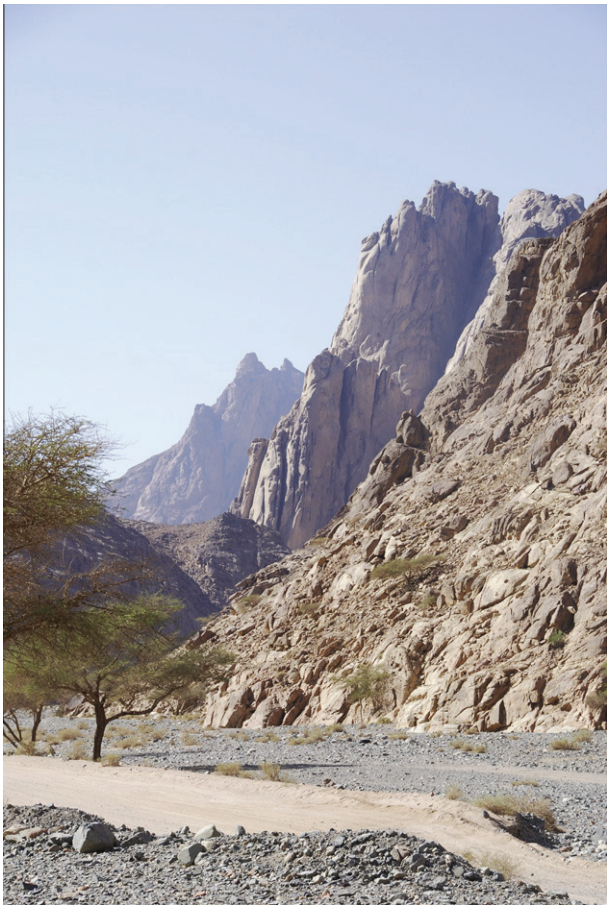

Fig. 12. View of the Dabbagh complex (577 ± 13 Ma: Aleinikoff and Stoeser, 1988), a typical alkali-feldspar granite in the northern part of the Midyan terrane that weathers out as a large granite massif rising high above the surrounding valleys.

4.2. Late Cryogenian–Ediacaran gabbro

Late Cryogenian–Ediacaran gabbro makes up a relatively small percentage of plutonic rocks in the ANS. Their geochronologic dataset (Appendix: five samples) is too small to draw a firm conclusion about their overall timing but the available data indicate a range of ~640 Ma to 540 Ma, implying that gabbro and granite magmatism overlapped in the ANS during the late Cryogenian–Ediacaran. Late- to post-tectonic gabbros are commonly distinguished by prominent layering (Coleman et al., 1972; Sadek, 1994; Greiling et al., 1994). Wherever observed, they are strongly discordant and appear to be among the youngest rocks in any given region of the ANS.

Notable examples of gabbro intrusions include the Thalath complex in the central Arabian Shield (Al-Muallem and Smith, 1987). The complex crops out as gabbro intrusions as much as 50 km across; several are circular to ovoid. Most are isotropic, but some have prominent inward-dipping gabbro–dunite layering and at least one has a core of gabbro and rim of anorthosite suggestive of a ring dike. The Lakathah complex in the southwestern Arabian Shield (Martin et al., 1979) is a nearly circular ring dike 10 km across composed of a pyroxenite–hornblendite core, an intermediate zone of diorite–gabbro, and an outer ring of syenite. The Wadi Kamal complex, NW of Yanbu' al Bahr in the northwestern Arabian Shield, is an irregular body of gabbro, anorthosite, and subordinate norite and leucogabbro forming southern and northern lobes connected by a trail of scattered intrusions. The complex is a significant PGM exploration target. The Ad Dawadimi (Harrat al Ji'lani) gabbro intrudes granite in the Ad Dawadimi terrane as an oval ring structure 7 km across (Al-Shanti, 1976). It comprises inward dipping layers of norite, gabbro, and minor amphibolite, which add up to a thickness of more than 3 km. Plagioclase–pyroxene gabbro cumulate predominates. The complex contains minor chromite and hosts silver veins belonging to the Ad Dawadimi silver district, but has no reported titaniferous magnetite or other metallic minerals.

The Akrarem complex in the Eastern Desert is a concentrically zoned mafic–ultramafic intrusion in the Eastern Desert composed of dunite and an outer zone of lherzolite–clinopyroxenite and hornblendite (Helmy and Mogessie, 2001). The dunite contains Cu–Ni–PGE mineralization with net-textured and massive lenses of pyrrhotite, pentlandite, and chalcopyrite, as well as Cr-magnetite. The complex is inferred to be mostly posttectonic, but is locally sheared, and some of the mineralization has been remobilized. Other late- to posttectonic mafic–ultramafic intrusions in the Eastern Desert, which clearly postdate "late tectonic" granitoids, include complexes of leucogabbro, anorthosite, and diorite, and alkaline granitoid (Akad and Abu El-Ela, 2002). One such complex comprises the Umm Gheigh gabbro in the southern part of the Sibai area, Central Eastern Desert, Egypt, which has an ID-TIMS U–Pb zircon crystallization of ~545–540 Ma (Augland et al., 2011). It is intruded by a dike dated at ~540 Ma, and together the rocks represent some of the youngest undeformed and posttectonic plutonic rocks in the ANS. The gabbro may be unrelated to other, slightly older layered gabbros in the area (Augland et al., 2011). Other distinctive late- to posttectonic gabbros occur along the Allaqi-Heiana suture zone as circular intrusions as much as 10 km across characterized by layers dipping 10–65° inward (Greiling et al., 1994; Sadek, 1994; Abdeen and Abdelghaffar, 2011).

4.3. Chemical characteristics and tectonic discrimination

Late Cryogenian–Ediacaran granitoids have been studied in the ANS because (1) they are spatially and genetically related to gold, REE, Ta, and Nd mineralization: and (2) their chemistry and isotopic compositions give important insight into the origin and evolution of the ANS crust.

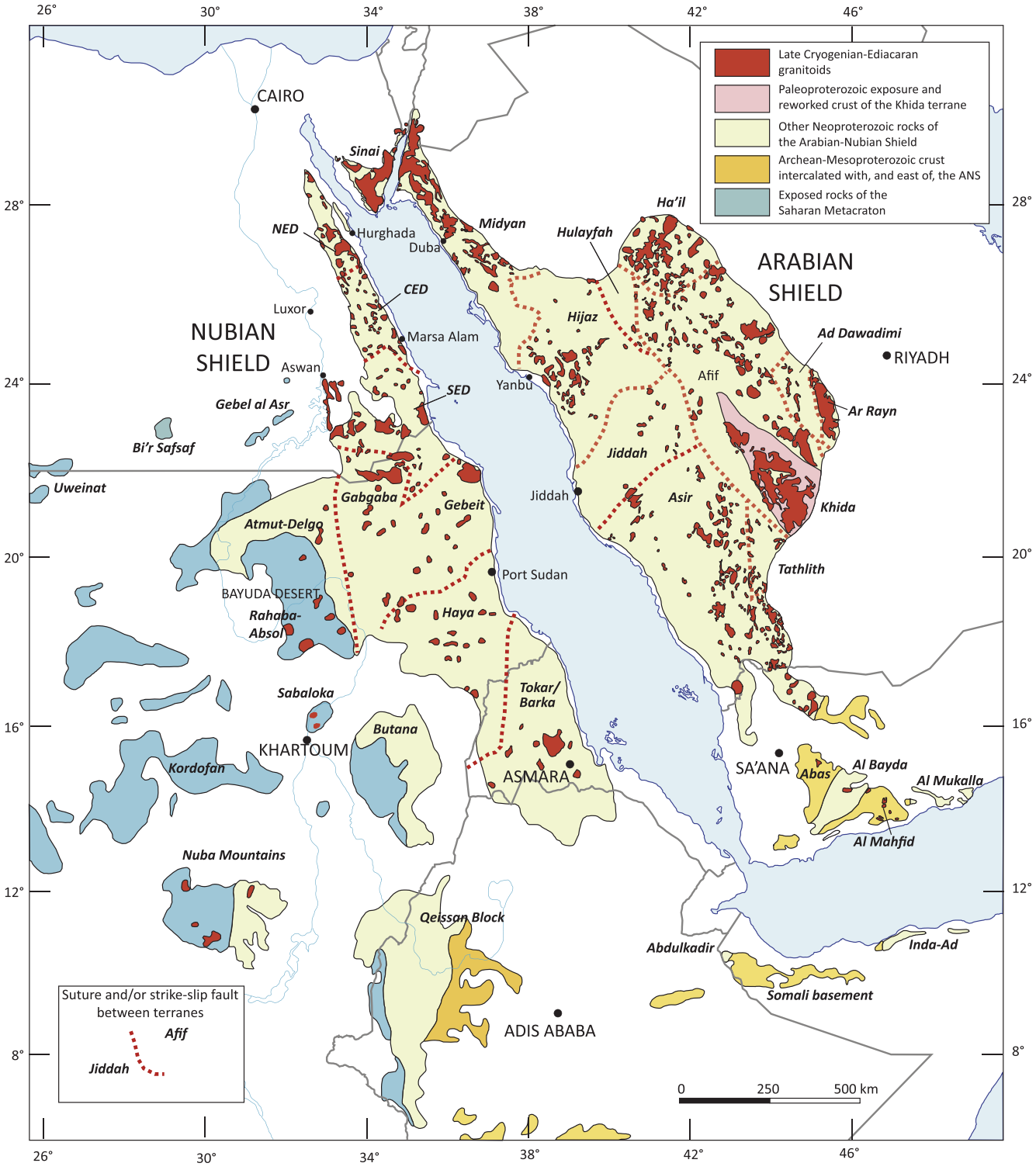

Fig. 13. Late Cryogenian–Ediacaran, late- to posttectonic, mostly discordant granitoids in the Arabian–Nubian Shield. Note the non-uniform distribution of the plutonic rocks with preponderance in the northern ANS.

Most ANS igneous rocks have lithologic associations (ophiolites, calc-alkaline igneous rocks, immature sediments) and isotopic compositions consistent with formation as juvenile continental crust. They have Nd model ages close to their crystallization ages (Stern, 2002; Stoeser and Frost, 2006; Moussa et al., 2008), mostly positive initial ε_{Nd}, and $^{87}Sr/^{86}Sr$ (Sr_i) close to that expected in evolving mantle of the same age (Fig. 14). This is particularly true for the TTG calc-alkaline rocks in the ANS. Initial $^{87}Sr/^{86}Sr$ above the standard mantle growth curves are found in middle to late Cryogenian and Ediacaran monzogranite, syenogranite, and alkali-feldspar granites and are notable, together with evolved Pb and Nd isotopes, in rocks from the Khida terrane (Stoeser and Frost, 2006) in which Paleoproterozoic crust was reworked during the Neoproterozoic.